Final Report

Air filtration plant of the M5 Tunnel. Determination of nitric oxide and nitrogen dioxide removal efficiencies

Prepared for
NSW RTA
By
Brendan Halliburton
Merched Azzi

EP EP117222 Final
November 2011

Enquiries should be addressed to:

Brendan Halliburton

Phone: 61 2 9490 5333

Email: brendan.halliburton@csiro.au

Merched Azzi

Phone: 61 2 9490 5307

Email: merched.azzi@csiro.au

Copyright and Disclaimer

Important Disclaimer

Report	Version	Date Uploaded
EP 117222	Final	1st November 2011
Revision	Description	Issue Date
01	Minor amendments	23rd November 2011

CONTENTS

TABLE OF FIGURES

TABLE OF TABLES

EXECUTIVE SUMMARY

CSIRO has been engaged by the Roads and Traffic Authority of NSW (RTA) to assess the performance of the M5 East Air Filtration System (AFP). This assessment includes the investigation of the removal efficiency of the nitric oxide (NO) and nitrogen dioxide (NO_2) mitigation technology (DeNOx) that has been installed within the AFP. This report presents the findings of this investigation.

To assess the DeNOx technology CSIRO has completed:

- A thorough scientific assessment of the measurement methodology and equipment that was used within the AFP to determine the NO and NO_2 removal efficiencies.
- A systematic experimental research program that has enabled the generation of NO and NO_2 removal efficiencies as well as quantifying the uncertainties associated with these efficiencies. This program utilised three scientifically different approaches.

The findings of this study are summarised as follows:

- The NO_2 removal efficiency for the DeNOx system:
    - Efficiency using time integrated techniques - 55% (8% uncertainty. Determined from two standard deviations from 23 measurements)
    - Efficiency using “real-time” Cavity Attenuated Phase Shift techniques (CAPS) - 55%

(Note at the time of writing this report a full analyses of the uncertainties associated with the CAPS measurements had not been completed. However, using the manufacturer"s specifications, in addition to published results in the open literature, it is expected that uncertainties associated with CAPS measurements would be significantly better than 5%.)

Time integrated and CAPS NO_2 measurement techniques were found to be the most reliable techniques with the smallest associated uncertainties. “Real-time” measurements using chemiluminescent analysers were found to have significantly larger associated uncertainties.

    - Efficiency using “real-time” chemiluminescent analysers (four instrument measurement technique) = 50% (100% uncertainty using a best case scenario from a numerical uncertainty analyses of the input data range)

- The NO_2 removal efficiency of the activated carbon sorbent has been determined independently from the DeNOx system. The NO_2 removal efficiency of the activated carbon alone was found to be 99% or greater over a wide range of gas flow rates.
- The NO_2 removal chemistry was found to evolve NO as a reaction product. NO evolution was observed to be spontaneous and the NO flux produced from the activated carbon continued for many hours after exposure to NO_2. This observed chemistry is well understood and has been documented in the open scientific literature.
- The NO removal efficiency of the AFP DeNOx technology has been determined using two separate techniques with efficiencies as follow:

  - Efficiency using time integrated techniques - 12% (5% standard deviation from 23 measurements)

  - Efficiency using “real-time” measurements - 12% (50% uncertainty using a worst case sensitivity analyses of the input data)

- The NO removal efficiency was found to be highly variable. The reason for the observed variability in efficiency is most likely a result of the chemistry associated with the catalytic sorption reactions occurring on the activated carbon. While this chemistry is complex, it is well defined in open literature. It is most likely that the NO and NO_2 sorption kinetics are parallel and competitive and as such may show non-linear kinetic behaviour. Catalytic behaviour with respect to NO_2 removal was observed as an “off-gassing” of NO from activated carbon after exposure to NO_2.

- The NO removal efficiency of the activated carbon sorbent has been determined independently from the DeNOx system. The NO removal efficiency of the activated carbon alone was found to be 56%

NO off-gassing was also observed when activated carbon was exposed to NO_2. Literature suggests that the two sorption chemistries of both NO_2 and NO produce a similar intermediate species. Literature has shown that this intermediate species consists of a carbon complex formed at the active site on the surface of the activated carbon matrix. Significantly more research is required if this complex chemistry is to be understood for the environmental conditions prevailing in the AFP.

- The removal efficiency of the DeNOx system installed within the AFP was measured to be less than the efficiency of activated carbon alone. It was observed that the most likely origin of this discrepancy arises from air leakage within and air leakage around the modules that are used to house and support the activated carbon.

1 INTRODUCTION

Air quality in the M5 tunnel is a high priority for Roads and Traffic Authority of NSW (RTA) and NSW Government. Air filtration is one possible method that can be used to remove gaseous pollutants and improve the air quality within automotive tunnels.

CSIRO has been engaged by the Roads and Traffic Authority of NSW (RTA) to assess the performance of the M5 East Air Filtration System (AFP). This assessment includes the evaluation of the nitric oxide (NO) and nitrogen dioxide (NO_2) mitigation technology (DeNOx) that has been installed within the AFP. To assess the DeNOx technology CSIRO has completed:

- A thorough scientific assessment of the measurement methodology and equipment that was used within the APF to determine the NO and NO_2 removal efficiencies.
- A systematic experimental research program that has enabled the generation of NO and NO_2 removal efficiencies as well as quantifying the uncertainties associated with these efficiencies.

This report presents the findings of this investigation.

2 OVERVIEW OF THE OPERATION OF THE INSTRUMENTATION USED WITHIN THE AFP TO DETERMINE OXIDES OF NITROGEN CONCENTRATIONS.

Before undertaking DeNOx efficiency measurements it is important to thoroughly assess the suitability, performance and limitations of the instruments that have been selected to undertake the proposed efficiency determinations.

It should be noted that initial NO and NO_2 efficiency measurements within the AFP were undertaken using Chemiluminescent NOx (CM) analysers. As such, the most detailed investigations, as well as the largest number of measurements, have been completed using CM instruments. Cavity Attenuated Phase Shift NO_2 analysers (CAPS) were acquired towards the completion of this study and after the limitations associated with CM analysers when operating in the AFP environment were identified. As such, a less rigorous NO_2 removal investigation has been completed using CAPS instruments and additional research is needed to provide the most accurate NO_2 removal efficiency data sets.

2.1 Chemiluminescence NOx analysers

2.1.1 Scientific Principles of the Chemiluminescence NOx analysers.

Chemiluminescence is the photon energy release that occurs during some chemical reactions. This phenomenon arises when a product molecule is created with increased electronic energy. This increased electronic energy state is energetically unstable compared to the normal electronic energy state found for the relaxed molecule. This unstable molecule subsequently “relaxes” to a reduced and more stable energy level. This energy loss occurs by either molecular collision with nearby molecules or through photon emission. Photon emission is the favoured mode of relaxation at lower pressures with the wavelength of the light produced being a function of the magnitude of the energy transitions that occurs during

the electronic relaxation process. The photon emission is associated with little thermal heat production. As gas pressure is increased the photon emission relaxation pathway is quenched as molecular collisions become the favoured relaxation mode.

Commercial NOx analysers utilise the CM reaction between excess ozone and nitric oxide at reduced pressure to detect the concentration of NO molecules in a gas stream. The reaction has been extensively studied (Johnson and Crosby, 1954; Clyne et al, 1963; Clough and Thrush, 1966; Glover, 1975) and is as follow:

$$O_{3(g)} + NO_{(g)} \rightarrow NO_{2(g)}{}^{*} + O_{2(g)} + 203kJ/mol$$

* electronically excited molecule.
(Johnson and Crosby, 1954)

The electronically excited nitric oxide molecule subsequently relaxes at reduced pressures as follows:

$$NO_{2(g)}{}^{*} \rightarrow NO_{2(g)} + hv$$

h = planks constant ($6.6x10^{34}$Js)
v = frequency of radiation (Hz)

In this reaction about 8% (Clough and Thrush, 1966) of the nitrogen dioxide is produced with increased electronic energy and this fraction is constant with reproducible quantum efficiency. Thus CM photon emission is a quantitative measure of the concentration of the nitric oxide reactant (Clyne et al, 1963; Glover, 1975; Bates, 1992).

The kinetics of this electronic relaxation is fast (Johnson and Crosby, 1954; Clyne et al, 1963; Glover, 1975) with the excited nitrogen dioxide molecule releasing photon energy in the spectral region from 600 to 2400nm (Clyne et al, 1963) during the process.

The chemiluminescent light intensity (I) is dependent upon temperature (T) and proportional to the concentration of nitric oxide and ozone but decreases according to the concentration of the carrier gas (M) due to quenching:

Equation 1

$$I = e^{-k/T}\frac{[NO][O3]}{[M]}$$

When a large excess of ozone is added to the NO sample the photon emission sensitivity to the ozone concentration diminishes. As such, the photon concentration is proportional to the concentration of nitric oxide in the gas sample, gas pressure, gas temperature and absolute concentration (of the carrier gas or quenching gas). Photon emissions are counted by a photon detection device such as a Photon Multiplier Tube (PMT). Hence, PMT response is only linear for constant pressure and temperature and with a large excess of ozone. Thus these parameters must be maintained constant during measurement. For scientific accuracy it should be noted that the concentration of M, the quenching gas, is a combination of all gases in the sample.

2.1.2 Commercial Chemiluminescence NOx analysers.

2.1.2.1 *Single Reaction Cell Chemiluminescence NOx analysers*

Commercial chemiluminescence NOx analysers, such as the instruments used in the AFP (Thermo Model 42i), directly measure the nitric oxide concentration of a gas sample. The concentration of total oxides of nitrogen is measured indirectly by way of a converter that reduces all oxides of nitrogen (other than nitric oxide) to nitric oxide. A simple diagram describing the operation of a chemiluminescent analyser is shown in Figure 2.1.

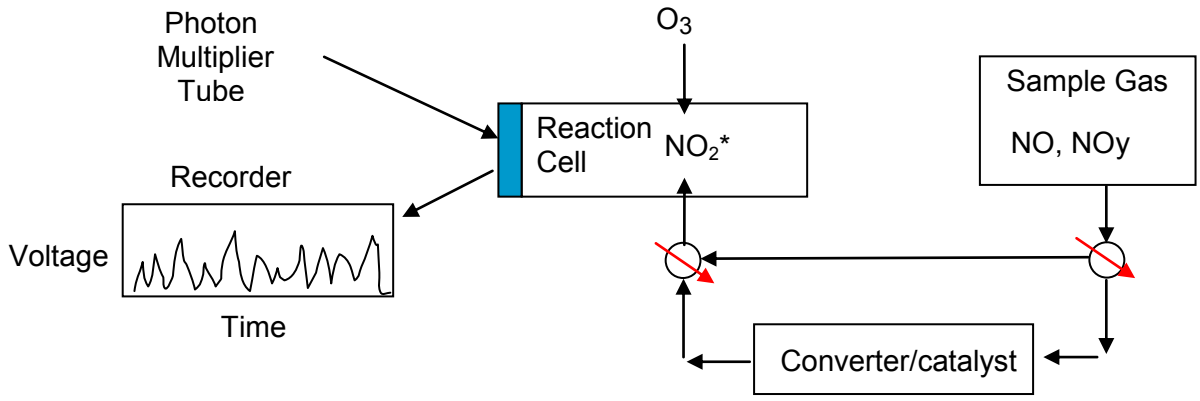

Figure 2.1. Principle of operation of the chemiluminescent analyser

* Includes carrier gas such as air

NOx reduction can be accomplished thermally, by heating the gas stream to a temperature in excess of 700°C or catalytically at lower temperatures. Converters are typically non selective which results in all oxides of nitrogen being converted to NO including nitrates, nitric acid (HNO_3), nitrous acid (HONO), organic nitrates [peroxyl acetyl nitrate (PAN), methyl peroxyl acetyl nitrate (MPAN), and peroxyl propionyl nitrate, (PPN)], and particulate nitrates. The strict scientific definition of the quantity measured by commercial „NOx" analysers while using a converter is a quantity called NOy, which is the term used to describe all oxides of nitrogen not just NOx. NOx is the scientific term used to define NO + NO_2 only. (Note The term "NOx analyser" and "NOx" will be used in this report to describe the CM measurements where the sample passes through the catalytic converter, or NOy, as this is consistent with commercial CM manufacturer"s terminology.)

Commercial "NOx" analysers assume that the other oxides of nitrogen are negligible in concentration compared to both NO and NO_2 concentrations. In most cases this is a valid assumption.

While the oxides of nitrogen can be thermally converted to NO at temperatures near 800°C, this process suffers from interference from gases such as CO. Therefore, most commercial "NOx" analysers use a catalyst to accelerate this conversion at lower temperatures. Commercial catalysts are typically carbon or molybdenum based. Catalytic converters can experience poisoning from a range of contaminants. Conversion efficiencies of all converters are generally less than 100%. As such this additional uncertainty must be reflected in NOx results.

Chemiluminescence cannot be used to simultaneously measure both NO and total nitrogen oxide concentrations within the same chemical reaction chamber. Modern chemiluminescent

NOx analysers designed for ambient monitoring have evolved to a single reaction cell system that alternately switchs gas flow between two gas circuits. One flow path passes the gas sample directly to the CM reaction cell (NO concentration determinations). The alternate circuit passes the gas sample through a catalytic converter (total nitrogen oxide determinations) prior to the gas entering the CM reaction cell. NO_2 concentrations are calculated from the difference between these measurements. Flow system artefacts and delays associated with the filling time of the reaction cell with the new sample must be correctly accounted for with this instrument design. Also transient peaks and troughs in gas concentrations may be "smoothed" depending upon the gas flow rate, reaction cell volume and the rate of change of gas concentration.

While the Photo Multiplier Tube (PMT) output of a NOx analyser is a continuous analogue signal, operation of a NOx analyser in gas switching mode constrains the output of the instrument to a series of discrete measurements spaced in time. The Nyquist-Shannon sampling theorem describes the minimum sampling frequency that is required for an analogue signal to be accurately re-created through discrete sampling and without artefacts such as aliasing. It states that the sampling frequency must be greater than twice the frequency of the analogue signal. If the NO_2 response of NOx analyser is considered using the Nyquist-Shannon theorem and with a discrete sampling period of 40 seconds for each NO_2 determination (frequency = O.025 Hz), then using this theorem, the minimum frequency that can be accurately resolved with the Thermo model 42i NOx analysers is 0.0125 Hz or a period of 80 seconds.

For measurements of nitrogen oxide concentrations in ambient air, the above sampling limitation is not significant as the rate of change of NOx is typically of the order of many minutes to hours. However, within the AFP the NOx signature is likely to be more transient and hence significant aliasing may be associated with these measurements. Correspondingly, it is important to experimentally determine the rate at which NO and NO_2 concentrations change within the AFP prior to DeNOx efficiency measurements.

2.1.2.2 *Dual Reaction Cell Chemiluminescence NOx analysers*

Dual reaction cell instruments are similar to single cell CM analysers except that two separate reaction cells and flow paths are used to separately but simultaneously measure the NO and NOx gas concentrations. Due to the parallel cell operation of these instruments dual reaction cell NOx instruments exhibit reduced sample collection timing and aliasing issues. A dual reaction cell "system" can be obtained by using two separate single reaction instruments, with one instrument measuring the NO concentration only and the other the NOx concentration. However, the use of two separate instruments increases the uncertainty of the NO_2 measurements due to the compounding of individual instrument uncertainties.

It should be noted that both single reaction cell and dual reaction cell analysers have performance limitations due to the flushing rate of the reaction cell. As such, chemiluminescent NOx (CM) analysers need to be optimised for increased flow if they are to elucidate highly transient NOx concentration signatures.

2.2 Cavity Attenuated Phase Shift NO_2 Analyser

The Cavity Attenuated Phase Shift (CAPS) NO_2 analyser utilises optical absorption to directly measure the concentration of NO_2. This is a relatively new instrument and to our knowledge this is the first instrument of this type deployed in this manner in Australia. These newly acquired instruments are the only instruments of this type in Australia at the time of this report.

The enhanced sensitivity of this instrument is achieved by an optically resonant cavity with a path length of approximately 3000m. A modulated light emitting diode (LED), with a narrow band wavelength of 430nm, is used as a photon source for the cavity absorption process. The LED is pulsed into the optical cavity and the photon "leakage", as a result of the optical cavity, is determined through the output voltage of a PMT. The PMT is used in conjunction with a narrow (10nm wide) band-pass interference filter that is optimised to the absorption wavelength of the target compound, in this case the 430nm absorption band of the NO_2 molecule.

During LED modulation the photon leakage of the cavity combined with photon absorption from gas molecules within the cavity produces a shift in the phase of the response signal measured by the PMT. By measuring the phase angle shift without NO_2 sample a baseline phase shift can be measured. During operation, NO_2 gas molecules within the cavity will increase photon decay and this will be reflected as a change in the PMT signal. This change in the PMT signal is a measure of NO_2 concentration. Using this principle it is possible to reliably measure NO_2 concentrations of less than 1ppb and up to 2000 ppb.

Due to the rapid sample filling rate the CAPS NO_2 analyser this instrument displays a fast response time of less than 1 second. Additionally, the CAPS measurement technique utilises a fundamentally based absorption technique and thus the CAPS NO_2 data represents the most accurate NO_2 concentration data for the AFP.

3 LOCATIONS OF FOUR CHEMILUMINESCENT NOx ANALYSERS WITHIN THE AFP.

Four CM analysers were initially installed within the AFP to measure the NO_2 removal efficiency within the plant. These instruments were installed in environmentally controlled cabinets that also contained a range of other instrumentation. Figure 3.1 displays the positions of the four measurement positions within the AFP. These measurement positions have been labelled "P1" to "P4". In this diagram the red arrows show the direction of the overall airflow while the blue arrows indicate the airflow through the NOx removal system.

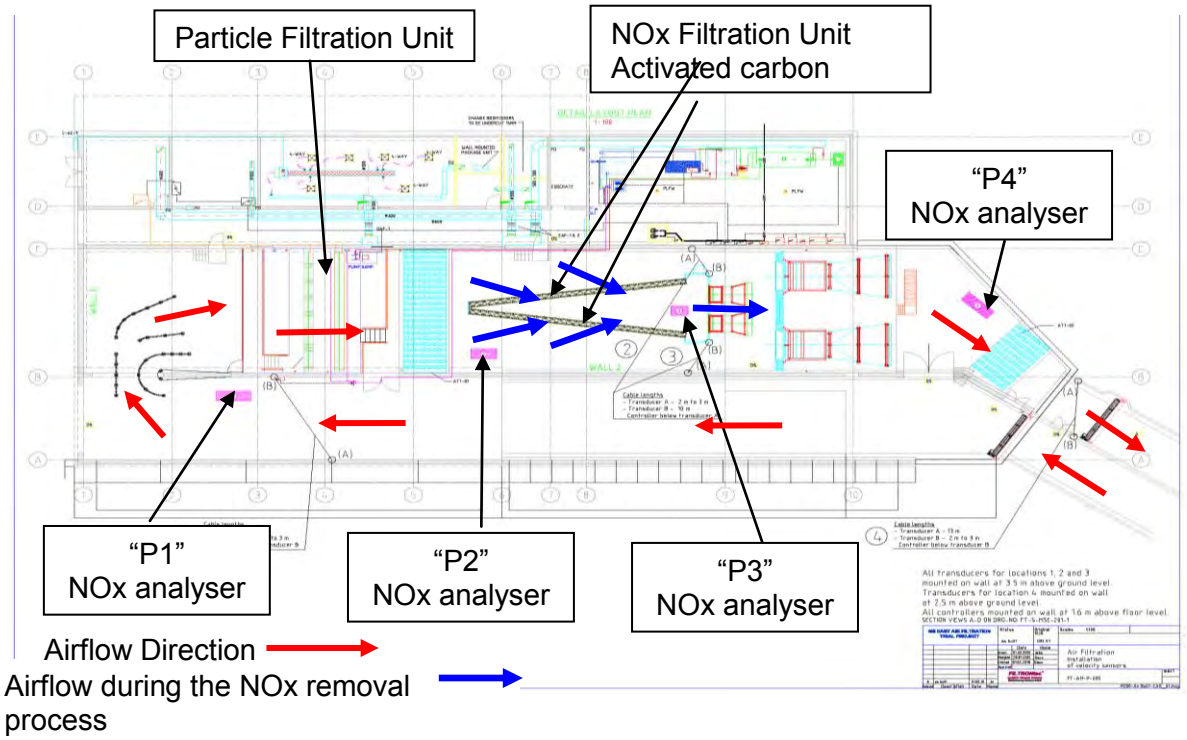

Figure 3.1. Positions of CM NOx analysers initially installed within the AFP

During normal operation, a portion of the particles in the air sample passing through the AFP accumulate in the particle filtration unit through electrostatic processes. NOx is removed by a separate filtration system that has been installed within the AFP but after the particle filter. The "DeNOx filtration system" (DeNOx) is formed by stacking more than 2000 activated carbon filled modules into a steel support structure. These modules comprise of stainless steel rectangular boxes and each module includes stainless steel wire mesh sections located at opposing ends of the box to allow air to flow through each module. A portion of the particle filtered air (50m^3/min) passing through the AFP is drawn into and through the NO_X removal modules that form the DeNOx system. After passing through the module the air is re-entrained back into the AFP airflow and eventually vented into the M5 tunnel. Figure 3.2(a) displays a single carbon module that has been filled with activated carbon while Figure 3.2(b) displays a portion of the DeNOx system.

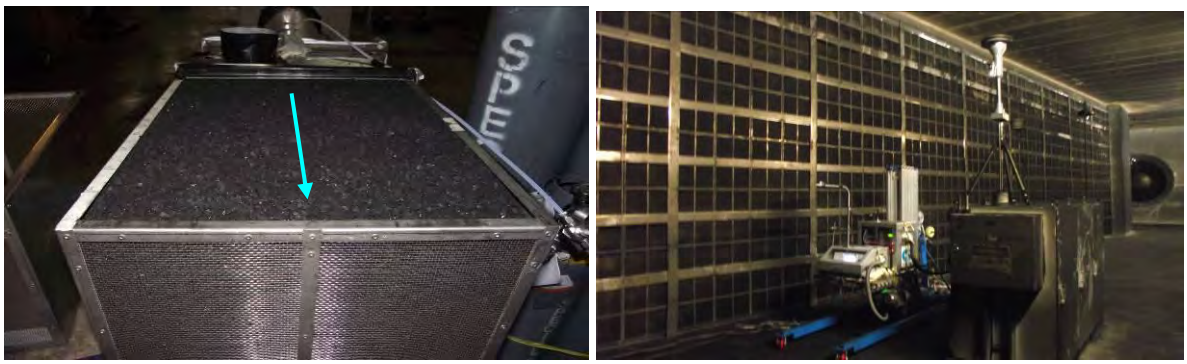

(a) (b)

Figure 3.2. A single activated carbon filled module (a) and a portion of assembly of these boxes stacked to form the DeNOx system (b).

Figure 3.2(a) displays a single activated carbon filled module. The direction of the airflow through the module is indicated by the blue arrow. Figure 3.2(b) also shows one of the

environmentally controlled cabinets (P2) used to contain the NOx and CAPS analysers. This cabinet can be observed as the large box located in the lower right corner of Figure 3.2(b). One of the Tapered Element Oscillating Microbalance (TEOM) particle measuring instruments was also housed within this cabinet and the sampling mast and other associated apparatus associated with this instrument can be seen above the cabinet. An Aerodynamic Particle Spectrometer can also be observed towards the centre of Figure 3.2(b).

4 PERFORMANCE ASSESSMENT OF THE CHEMILUMINESCENT NOx ANALYSERS.

Before the NOx measurements were undertaken at the AFP detailed evaluations of the four Thermo 42i NOx analysers, the zero air generators and calibration gas mixing instruments were completed. The assessment of the zero air and gas calibration mixer is included in Appendix 2.

These assessments consisted of:

- The determination of the response time of the Thermo 42i NOx analysers
- Multipoint calibrations to assess the linearity of the response of each instrument to assess the uncertainty associated with output linearity.
- Regular calibrations to assess instrumental precision.
- Longer term calibrations to assess instrument drift.
- Periodic comparison of the zero air generator to a zero air reference cylinder.
- Flow calibration of the gas mixer unit to assess linearity, drift and precision.

4.1 Response time of the Thermo model 42i NOx analysers

The response time of the four CM instruments installed within the AFP to a step change in gas concentration is shown in Figure 4.1.

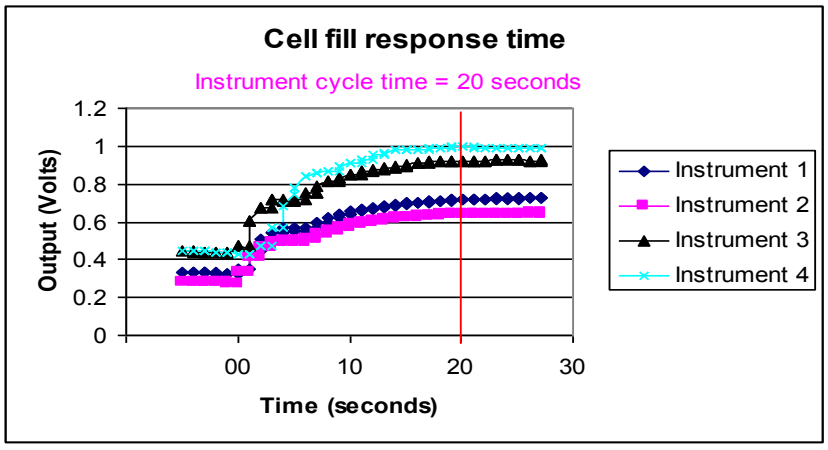

Figure 4.1. Response times of the four Thermo 42i NOx analysers installed within the AFP

To obtain these data displayed in Figure 4.1, the four instruments installed within the AFP were programmed to continuously measure either NO or NOx without sample switching. Instruments identified as “1” and “2” in Figure 4.1 were programmed to measure NO while instruments identified as “3” and “4” were programmed to measure NOx. Each instrument was initially challenged with a constant concentration gas mixture of NO and NO_2 until the output stabilised. The stable concentration can be seen by the steady readings from each

instrument leading up to time “00”. The gas stream was then quickly and simultaneously changed to an increased but steady concentration of NO and NO_2. This change was completed by way of solenoid valving that simultaneously switched between the two gas streams. These valves were located at the sample port to each instrument. The response of the output voltage of each instrument was then monitored and these results are displayed in Figure 4.1. These data show that the filling of the reaction cell of these instruments requires nearly the entire 20 second period of the normal operation of the gas switching cycle to completely flush the reaction cell and obtain an accurate steady gas concentration result.

Thus to obtain accurate NO_2 concentration measurements a minimum of 40 seconds of steady NO or NOx flow at constant gas concentration is required. Additionally, these data indicate that the time period over which the NOx instrument acquires the concentration data for the calculation of the reported result is only the short steady period just prior to gas sample switching.

4.2 Output linearity Thermo model 42i NOx analysers

To assess the linearity of the Thermo 42i NOx analysers periodic multipoint calibrations using a NATA certified (Coregas) calibration mixture were undertaken. An example of these data is shown in Figure 4.2.

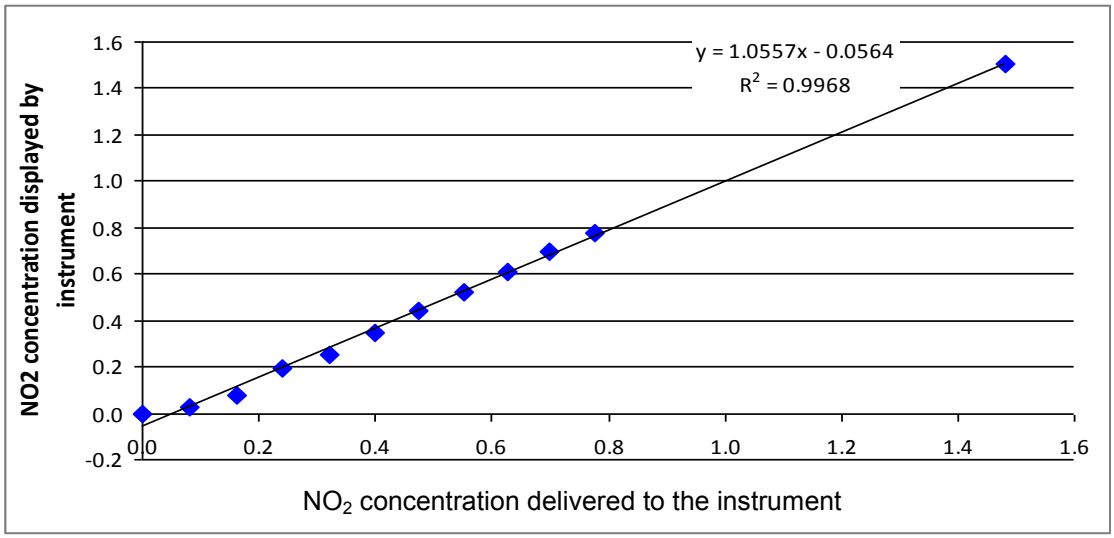

Figure 4.2. An example of output signal linearity from a Thermo 41i NOx analyser.

The data set displayed in Figure 4.2 show the linearity in output response of one of the Thermo 41i CM analysers. During these measurements the instrument was challenged with accurately prepared calibration mixtures of NO_2 gas at varying concentrations. In this measurement NO_2 calibration gas (Coregas NATA certified gas mixture) was accurately diluted with zero air using an Environics 6100 mixer to achieve the gas concentrations shown in this Figure 4.2. To eliminate the impact of gas mixer non-linearity, the gas mixer was used only as a flow controller and not used to determine the mixing ratio. The delivered concentrations were determined volumetrically using a precision primary volumetric standard (Bios International, Defender 5100) that was calibrated by the manufacturer.

These data reveal that the uncertainty of the Thermo 42i NOx analyser was within the manufactures range of 1% uncertainty with respect to linearity.

4.3 Instrumental precision and Drift of the Thermo model 42i NOx analysers

During all NOx concentration measurements the Thermo 42i NOx analysers were routinely calibrated against a NOx reference gas mixture at a known and constant concentration. This was achieved using a NATA certified (Coregas) calibration mixture diluted with zero air through a dilution system referenced to a primary volumetric standard (Bios International, Defender 510 calibrated by manufacturer). The longer term drift of these instruments was determined to vary between 4% and 7%, depending on the instrument. However, the span drift over one day was measured to be 1%.

4.4 Uncertainties associated with NOx Measurements

Additional validation measurements were undertaken on each of the four Thermo 42i NOx analysers, the gas mixing unit and zero air generator. These validation measurements included measurements to assess parameters such as the precision of each device and the long term drift. The results of these validation measurements are presented below in Table 4.1 and these uncertainties have been used to calculate the uncertainties associated with the NO and NO_2 removal efficiencies.

Table 4.1. Sources of uncertainties associated with NOx measurements.

SPECIFICATION	PERFORMANCE
SPAN LINEARITY	± 1%
ZERO DRIFT	± 1%
SPAN DRIFT (Daily)	± 1%
ZERO DRIFT (LONG TERM)	± 1%
SPAN DRIFT (LONG TERM)	4% to 7%
INSTRUMENT NOISE	1%
GAS MIXER UNCERTAINTY	4% to 8%
NO_2 CATALYST CONVERTER EFFICIENCY	1% to <5%
ROUNDING OF ANALOGUE TO DIGTAL CONVERSION	0.1%
CALIBRATION GAS (Coregas speciality standard)	2%
TIME DELAY THROUGH DeNOx	1.5%

The uncertainties listed in Table 4.1 are a combination of measured uncertainties associated with the instruments used in this study as well as the manufacturer‟s reported uncertainties in the case of calibration gases concentrations and analogue to digital conversions. It should be noted that not all of these uncertainties are additive during difference based efficiency calculations.

5 “REAL TIME” MEASUREMENTS WITHIN THE AFP.

The behaviour of NO and NOx concentrations in the AFP are critical parameters for evaluating the suitability of the CM NOx measurement methodologies. As identified in sections 2.1, 2.1 and 4.1, the Nyquist-Shannon sampling theorem stipulates that the Thermo 42i NOx analyser will be unable to resolve NO_2 concentration changes shorter than 80 seconds if signal aliasing is to be avoided. Consequently, it is essential to measure the time dependence of the NO_2 signature within the AFP. To investigate the temporal behaviour of NO and NOx concentrations within the AFP, a Monitor Labs 8840 (ML8840) dual reaction-cell NOx analyser was utilised.

5.1 The Time Dependence of the NO and NOx Signature at the AFP.

Figure 5.1 displays an example of these measured NO and NOx concentrations as well as calculated NO_2 concentrations within the AFP using a ML8840 analyser. In this example, a half hour period of data is shown. In addition, a portion of these data are shown at increased resolution.

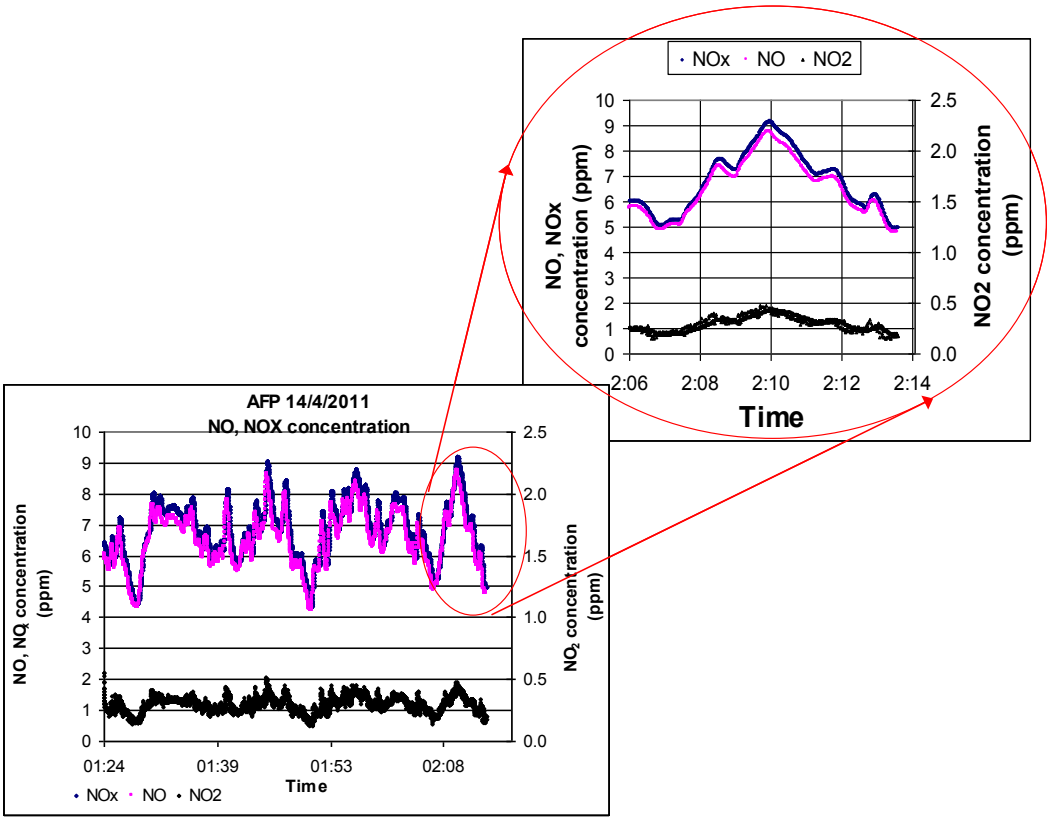

Figure 5.1. AFP measurements using the Monitor Labs 8840 NOx analyser.

Data sets presented in Figure 5.1 represent the time series of NO and NOx concentrations that are exhausted from the M5 automotive tunnel roadway into the AFP. This figure also includes the calculated NO_2 time series and these data are shown as black data points. It should be noted that the Monitor Labs 8840 NOx analyser is an analogue instrument and so is free from aliasing. However, to minimise aliasing uncertainties associated with electronic recording these analogue data, these data were digitally recorded at 0.3Hz resolution. The analyser was positioned after the particle filter but before the DeNOx system within the AFP.

The results of these measurements show rapid changes in NO and NOx gas concentrations. Both the absolute concentrations as well as the ratio of these gases changed rapidly and within the normal 20 second measurement period of the Thermo 42i when these instruments are operated for ambient monitoring or Switched Flow Mode (SFM).

5.2 The Time Dependence of the NO_2 Signature at the AFP.

The CAPS instruments used in this study have response times of 1 second and hence uncertainties arising from signal aliasing are reduced compared to CM analysers. Figure 5.2 shows and example of the NO_2 signature presented to the AFP from the M5 tunnel.

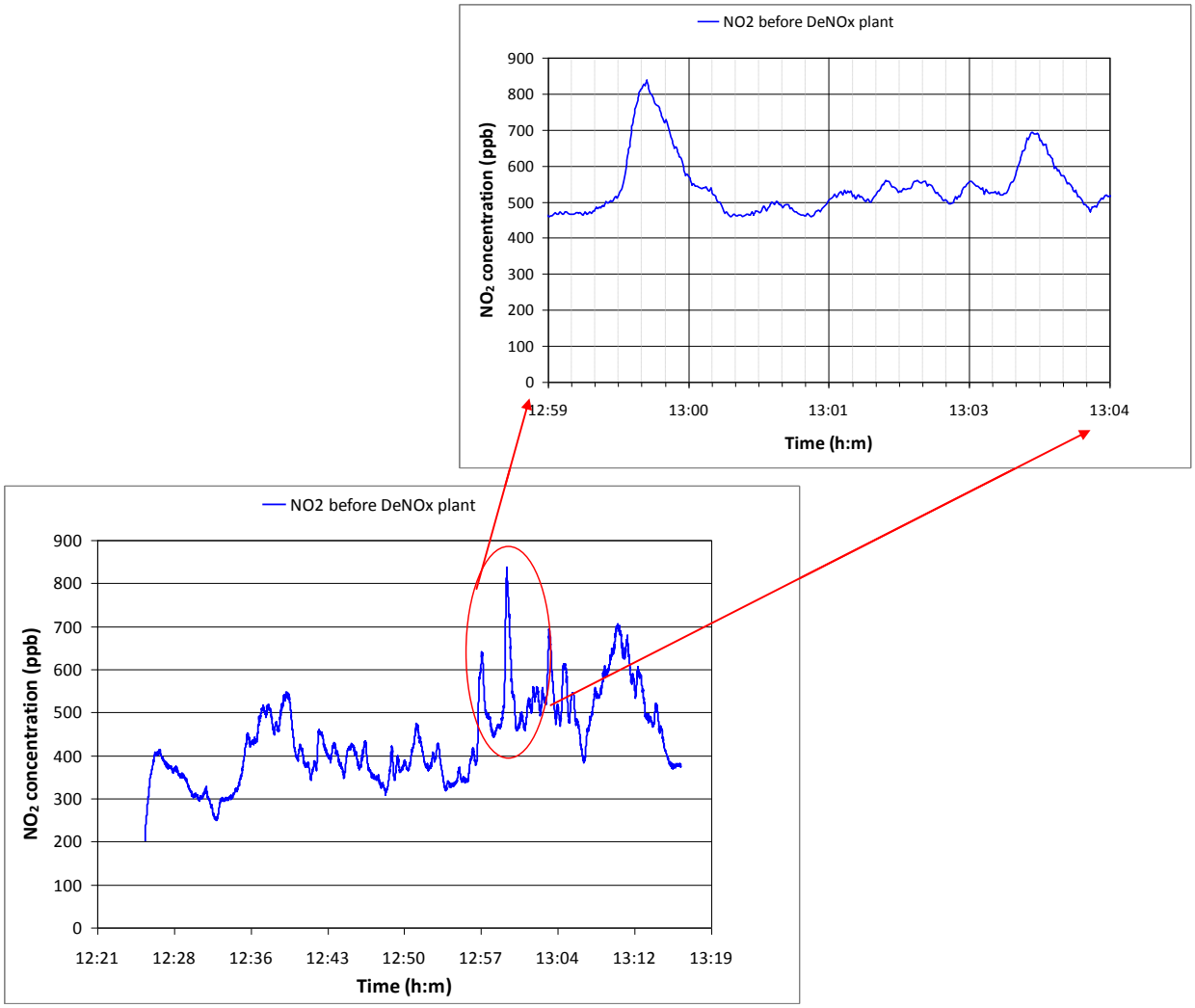

Figure 5.2. AFP measurements using the Aerodyne Research CAPS NO_2 analyser.

An example of the NO_2 concentration signature presented to the DeNOx system from the M5 tunnel and measured by the CAPS analyser are displayed in Figure 5.2. These data have been measured with a sampling rate of 1Hz. The reader is focussed to the CAPS NO_2 concentration trace between 12:59:30 and 12:59:40 where a NO_2 "spike" can be observed. It is likely that this NO_2 "spike" is a result of emissions from a single diesel vehicle or a number of diesel vehicles at close proximity. During the time period under analyses the CAPS analyser measured a NO_2 concentration increasing from approximately 500ppb at 12:59:30 to greater than 800ppb at 12:59:40. Furthermore the NO_2 concentration reduced to approximately 500ppm after a further 20 seconds of sampling. Given that a 40 second time period is required for CM analysers to report one NO_2 measurement, these transient NO_2 data would not be discernable when using a CM analyser in the normal ambient measurement mode where the instrument alternately switches between NO and NOx flow circuits.

Additionally, if the measured NO and NOx concentration signatures displayed in Figure 5.1 are compared to the measured NO_2 signature displayed in Figure 5.2, then these data in Figure 5.2 suggest that the true rate of change of NO and NOx concentration are more aligned with the behaviour of the NO_2 concentration signature shown in Figure 5.2. Furthermore, if the NO_2 signatures displayed in Figures 5.2 and 5.1 are compared then it can

be observed that much of the transient detail shown in Figure 5.2 is reduced in Figure 5.1. Given that the rate of change of the NO and NOx concentration within the AFP is likely to be greater than the time resolution of the Thermo 42i CM analysers, it is likely that the calculation of NO and NOx removal efficiencies, using real time measurement techniques, will include large experimental uncertainties. As such, these results indicate that an alternative experimental technique will be required to obtain accurate NO and NOx removal efficiencies for the AFP environment.

5.3 The Implications of the Transient AFP NOx Signature for "Real Time" NOx Removal Efficiency Measurements.

The four Thermo 42i CM analysers installed within the AFP at locations shown in Figure 3.1 were initially operated using the normal NATA accepted ambient monitoring methodology (that is switched flow mode) with six minute averaging periods. Correspondingly, it is instructional to evaluate the influence of the observed transient NOx signature within the AFP with respect to the uncertainties associated with NOx removal efficiency results.

Figure 5.3 displays NO_2 concentration data, labelled as "dual NOx analysers NO_2 concentration", which has been calculated using two Thermo 42i CM NOx analysers that were operated in parallel. For this example one instrument measured the NO concentration while the other measured the NOx concentration. A second NO_2 concentration signature, labelled "Flow switching mode NO_2 concentration", has also been included and this represents what would be reported by a single NOx analyser operating with the shortest averaging time.

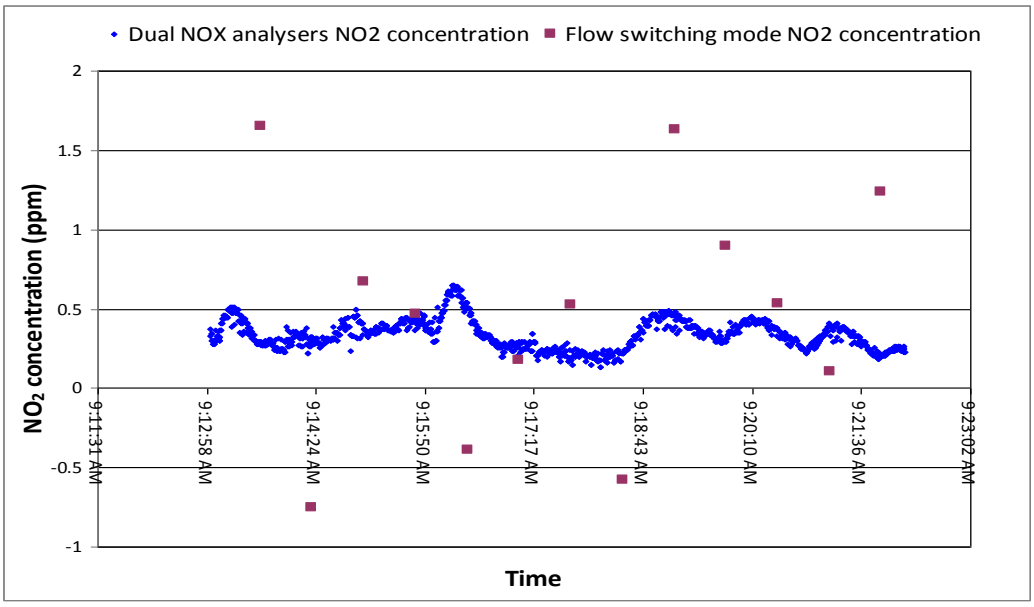

Figure 5.3. Comparison between NOx measurements using tandem CM analyser and a single CM analyser.

The NO_2 concentration signature displayed as blue data points in Figure 5.3 has been calculated from the difference between NO and NOx outputs from two concurrently sampling Thermo 42i CM analysers. Each instrument was co-located within a temperature controlled cabinet and sampled the gas stream within the AFP through a common sampling manifold. Each instrument was calibrated before, during and after these measurements by periodic addition of either a zero gas or a calibration gas mixture (Coregas NATA certified standard)

directly into the sampling manifold. The calibration and zero gas flows were maintained at flow rates greater than that of the sample flow rate of the instrument. These NO_X analysers were operated at the maximum instrumental sampling rate and these output voltages were recorded at 0.3Hz using an external electronic logger. Unfortunately, the voltage output of the NOx instruments was not a true analogue output from the PMT but rather an electronically synthesised voltage output from a Digital to Analogue (DA) converter. Thus additional uncertainty is associated with these additional digital conversions compared to the analogue data reported in Figure 5.3. However, it is expected this additional uncertainty would be small.

While these "real-time" NO_2 data display similar transient concentration behaviour as displayed in Figure 5.1 this is not the case for calculated Switched Flow Mode (SFM) data. These SFM data display extremely large NO_2 concentration fluctuations as well as significantly negative NO_2 concentrations and generally exhibit different behaviours to the measured "real-time" data set shown as blue data points. The behaviour of these SFM data is what would be expected from measurements that includes aliasing and time alignment errors. Given that NO_2 removal efficiency is calculated by difference of two CM NOx instruments, then the uncertainty associated with NO_2 removal efficiency calculations will be significantly greater than the uncertainties suggested in Figure 5.3. These uncertainties will be especially large for the case where two CM NOx analysers operate in SFM with one CM analyser upstream of the DeNOx system and one CM analyser down stream of the DeNOx system and without time alignment of the data sets.

This investigation has highlighted the extreme importance of thoroughly investigating the influence of the characteristics and behaviour of the gas to be analysed as well as the influence of these behaviours upon the measurement methodology and instrumental operation. Data reported in this section clearly show that it is essential for dual NOx analysers be used for CM NO_2 measurements within the AFP if scientifically robust "real time" NO_2 removal efficiency data are to be produced. As such, the Thermo 42i CM analysers have not been used in the normal NATA certified ambient monitoring mode for this study. Correspondingly, all subsequent NOx measurements discussed within this report have utilised alternative measurement methodologies. Additionally, the CM NOx analyser limitations identified in this section may have implications in other situations that include rapid concentration changes.

5.4 Measurements using Dual Chemiluminescent NOx Analysers.

Two dual reaction cell NO_X analysers were not available for this study. As such, four Thermo 42i CM NOx analysers were operated as two pairs of instruments with one instrument from each pair assigned to measure NO and the other instrument assigned to measure NOx. The NOx analysers were located at positions identified as "P 2" and "P 3" in Figure 3.1. As discussed in 5.3, the calibration of all four instruments was completed "online" with the calibration gas directly metered into the sample manifold.

Figure 5.4 displays an example of the raw NO, NOx voltages that were recorded from four NOx analysers during a 3 hour period.

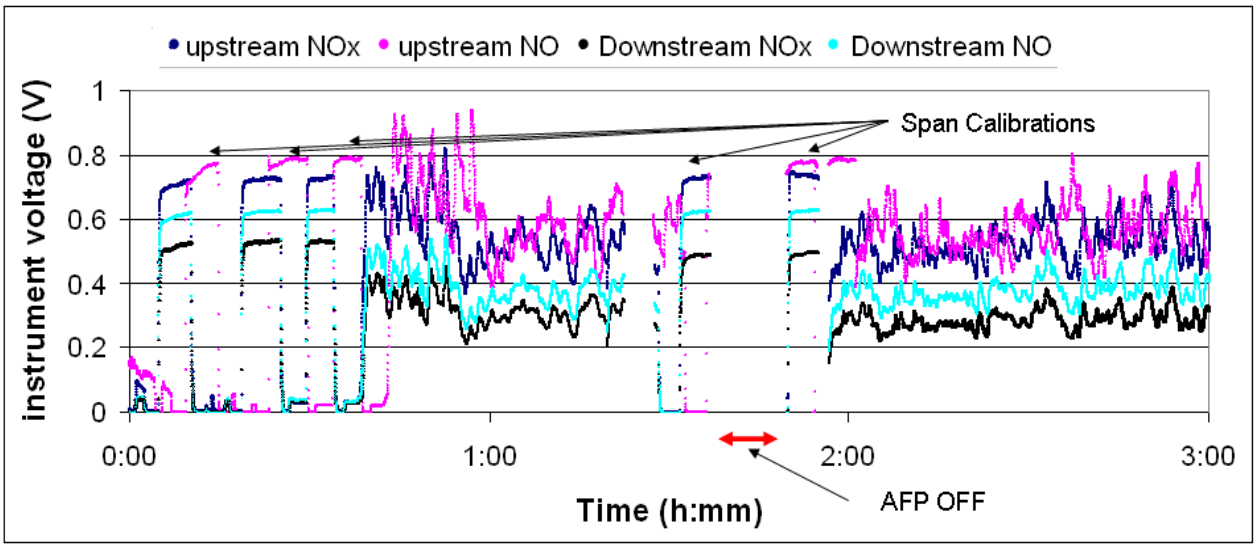

Figure 5.4. Four examples of raw voltage data produced by the Thermo 42i NOx analysers.

Data presented in Figure 5.4 are examples of the raw voltage data sets generated for each of the four Thermo 42i NOx analysers. For each of the four instrument traces, five calibration peaks can be seen corresponding to each instrument being challenged with NATA certified (Coregas) NO/NO_2 gas mixture that was accurately diluted with "zero" grade air. Between the regular NOx span calibration periods these instruments were challenged with zero air to determine baseline voltages. These span and zero calibrations were used to scale the raw voltage data from each instrument and generate NO and NOx concentrations. Span and zero calibrations were completed before and after each set of measurements and instrumental drift accounted for over the measurement period. These regular span and zero calibrations were also used to assess the longer term drift of the instrumentation. Examples of the NOx concentration data are shown in Figure 5.5.

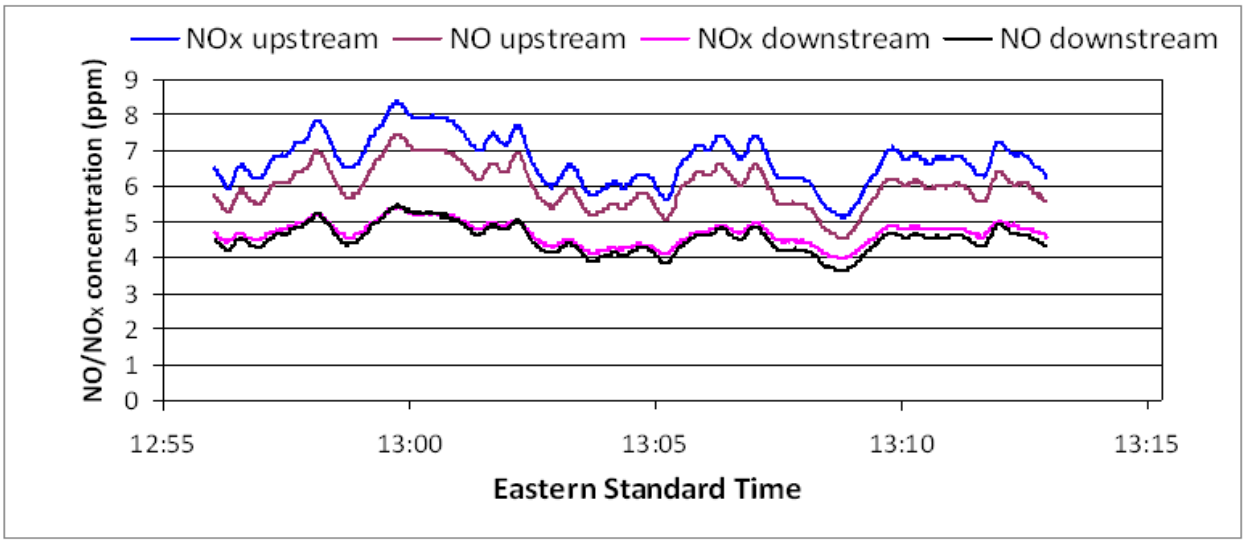

Figure 5.5. Example data of NO and NOx concentrations before and after the DeNOx system.

Figure 5.5 displays examples of the NO and NOx concentrations that are measured by the pairs of NOx analysers installed at "P 2" and "P 3". These data sets have been time aligned with the upstream NO and NOx measurements offset by 10 seconds to account for the

spatial separation of each pair of NOx analysers. These data clearly show that the fraction of NO in the NOx sample is not constant and as such implies that the fraction of NO_2 in the NOx sample is variable. This result is examined further in Figure 5.6 where the fraction of NO and NO_2 in each of the NOx samples is displayed.

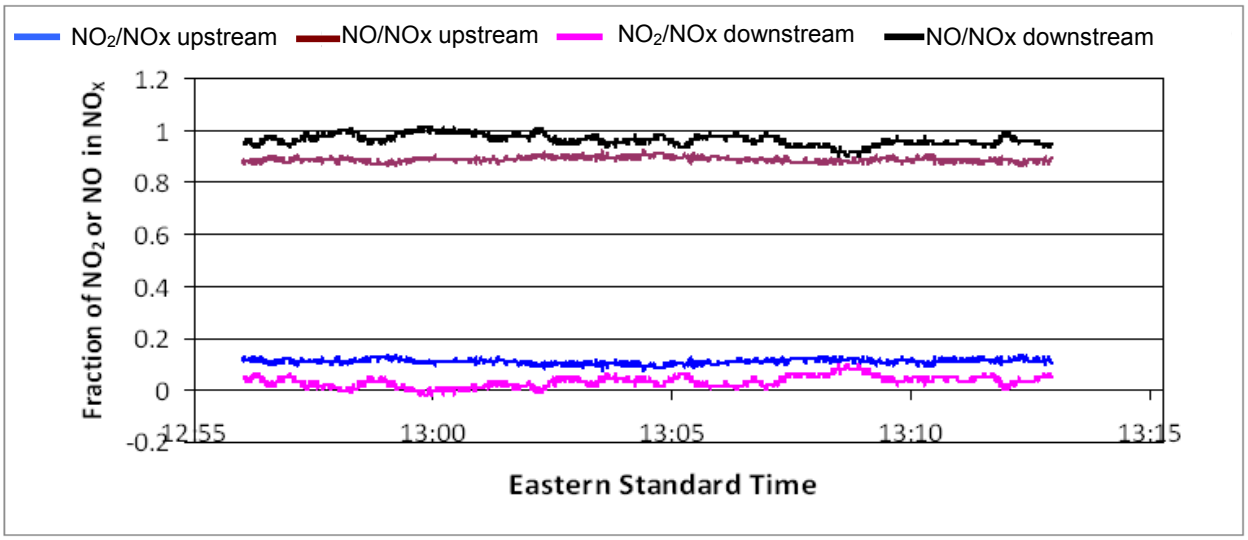

Figure 5.6. Fractions of NO_2 and NO and NOx before and after the DeNOx system.

These data displayed in Figure 5.6 highlight the large variability of the fraction of NO in the measured NOx sample both before and after the DeNOx system. Consequently, a large degree of uncertainty is also included in the NO_2 concentrations calculated by these instruments. This observation clearly highlights the experimental difficulty and the large degree of uncertainty associated with measurements of small and variable NO_2 concentrations using CM instruments. Furthermore, these uncertainties are magnified when differential efficiency measurements are undertaken using CM analysers even when these instruments are time aligned. These calculated "real time" NO and NO_2 removal efficiencies measurements further explored in Figure 5.7.

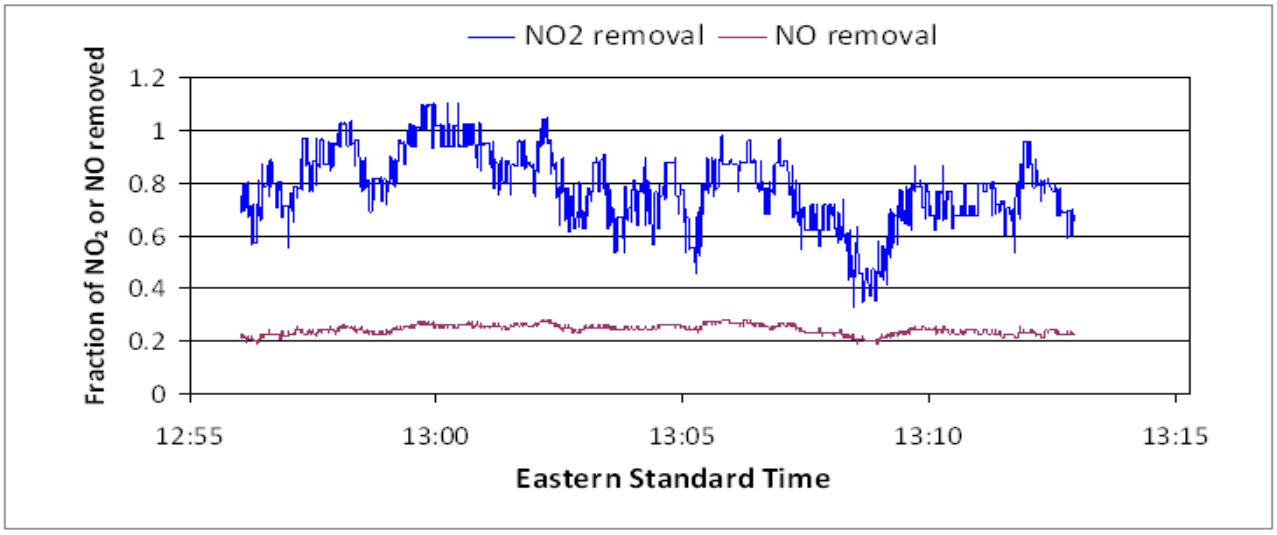

Figure 5.7. Differentially calculated real time" NO and NO_2 removal efficiencies.

Figure 5.7 displays examples of the NO and NO_2 removal efficiencies that have been calculated by the difference between the NO and NO_2 concentrations of the upstream and

downstream analysers located at P 2 and P 3. These data have been calculated on the basis of:

$$\frac{\text{Upstream } NO_2 \text{ concentration - downstream } NO_2 \text{ concentration}}{\text{Upstream } NO_2 \text{ concentration}}$$

While these calculated NO removal efficiencies remain relatively constant over the time period of these example data, this is not the case for these NO_2 removal efficiency data which display widely varying efficiencies. These NO_2 removal efficiency data include calculated efficiencies that are greater than unity, a result that is clearly erroneous. Additionally, these NO_2 efficiency data display efficiencies that are relatively small with values of the order of 40% removal being observed. These NO_2 efficiency data also display an apparent "stepped" trend in the data with a relatively large minimum resolution. It is likely that this apparent large "step wise" change in the NO_2 efficiency originates from the minimum combined resolution of the analogue to digital and then digital to analogue conversions process that is occurring at each CM analyser. The variability in these NO_2 efficiency data clearly highlight the large degree of uncertainties associated the CM measurements even though each instrument has an individual precision of a few percent during calibrations. The overall results of these "real-time" efficiency measurements are summarized in the following section.

5.5 Uncertainty calculations associated with of "Real Time" Chemiluminescent NO_2 and NO Removal Efficiency Results

Due to the transient nature of the NOx concentration signature presented to the DeNOx system the measurement of NO and NO_2 removal efficiencies using the "real time" technique and CM analysers proved to be most challenging. In addition, as identified in Section 5.2 it is likely that the rate of change in concentration of NO and NOx will exceed the response time of the Thermo 42i NOx CM analyser.

NO_2 removal efficiency calculations using CM analysers and "real-time" difference methodology inherently include large uncertainties in the calculated results. These large uncertainties arise even with very small individual instrumental uncertainties (2.1% for the statistical uncertainty associated with real-time measurements for a four CM instrument combination with gas mixer, CM instrument, calibrations and analogue to digital converter). The large uncertainties arise due to amplification and the cascade of uncertainties that occurs during NO_2 removal efficiency calculations in addition to the relative small fraction (~10%) of NO_2 in the NOx gas sample.

The assessment of "real-time" CM uncertainties associated with these NO_2 removal efficiency calculations have been assessed using a numerical uncertainty analyses where all input parameters involved in the efficiency calculation are varied over their respective uncertainty bands. This method provides a worst case uncertainty evaluation as all relative uncertainties are assessed in an additive manner in the final efficiency calculation. This method does not consider the case where systematic errors may cancel, as may be the case for difference calculations or relative changes, and does not include statistical improvement in uncertainties due to multiple measurements. However, this method of uncertainty assessment is very useful in understanding how input uncertainties propagate through the calculations as well as assessing the sensitivity of calculated results to the input data sets.

The difference calculation presented in section 5.4 requires CM input data sets for both the upstream and downstream NO_2 concentrations. However, CM analysers generate these NO_2 concentrations through the gas concentration differences as shown below.

$$\frac{(\text{Upstream (NOx - NO) concentration}) - (\text{downstream (NOx - NO) concentration})}{\text{Upstream (NOx - NO) concentration}}$$

Numerical analyses of this calculation indicate that the uncertainties associated with NOx and NO concentrations compound with difference calculations. Worst case NO concentration uncertainties are of the order of 10% depending upon the particular CM analyser while worst case NOx uncertainties are of the order of 20%. Numerically analysing these uncertainties though the worst case scenario the uncertainty associated with reported NO_2 "real time" efficiencies calculates to an order of 200%. At best, the uncertainties associated with the calculated NO_2 efficiencies are of order of 100%. Correspondingly, the best the uncertainties associated with the calculated NO efficiencies are of order of 50%.

5.6 Summary of "Real Time" Chemiluminescent NO_2 and NO Removal Efficiency Results

Table 5.1. "Real Time" Chemiluminescent NO_2 and NO Removal Efficiencies

NO and NO_2 Removal Efficiency Summary	
Number of measurements days	27
Number of measurement hours	118
Average NO_2 removal (all measurements)	50%
Overall NO_2 best case uncertainty[1]	Up to 100%
Overall NO_2 worst case uncertainty[1]	Up to 200%
Average NO removal (all measurements)	12%
Calculated NO uncertainty[1]	Up to 50%

[1] Uncertainty calculated from the combination of all contributing uncertainties associated with the calculation of the removal efficiency.

5.7 Conclusion

Due to the highly transient nature of the NOx concentration signature presented to the DeNOx system as well as the relatively large magnitudes of NO and NOx concentrations compared to the NO_2 fraction, the uncertainties associated with NO_2 concentration measurements are significantly greater than for NO and NOx measurements. When these NO_2 data are used to calculate NO_2 removal efficiencies the associated uncertainties are further magnified. The NO_2 removal efficiencies for these "real time" measurements were determined to be at best of the order of 100% and at worst 200% while the uncertainty associated with NO removal efficiency was determined to be of the order of 50%. Due to these large uncertainties alternative measurement methodologies were developed and alternative instruments acquired to more accurately fulfil the obligations of this study.

5.8 NO_2 Removal Efficiency Measurements using the Cavity Attenuated Phase Shift Instrumentation.

As detailed in section 2.2 Cavity Attenuated Phase Shift (CAPS) is a new measurement technique and unlike CM instruments, the CAPS instrument directly measures NO_2 gas concentrations. CAPS instruments were installed at positions labelled as “P 2” and “P 3” in Figure 3.1. These instruments were operated as calibrated by the manufacturer (Aerodyne Research, USA) and these calibrations validated “on-line” by the same calibration methodology as used for the CM instruments. It should be noted that the CAPS instruments were acquired after the elucidation of the operational and uncertainty limitations of the CM analysers.

Figure 5.8 displays an example of the CAPS NO_2 concentration data measured on 9/8/2011.

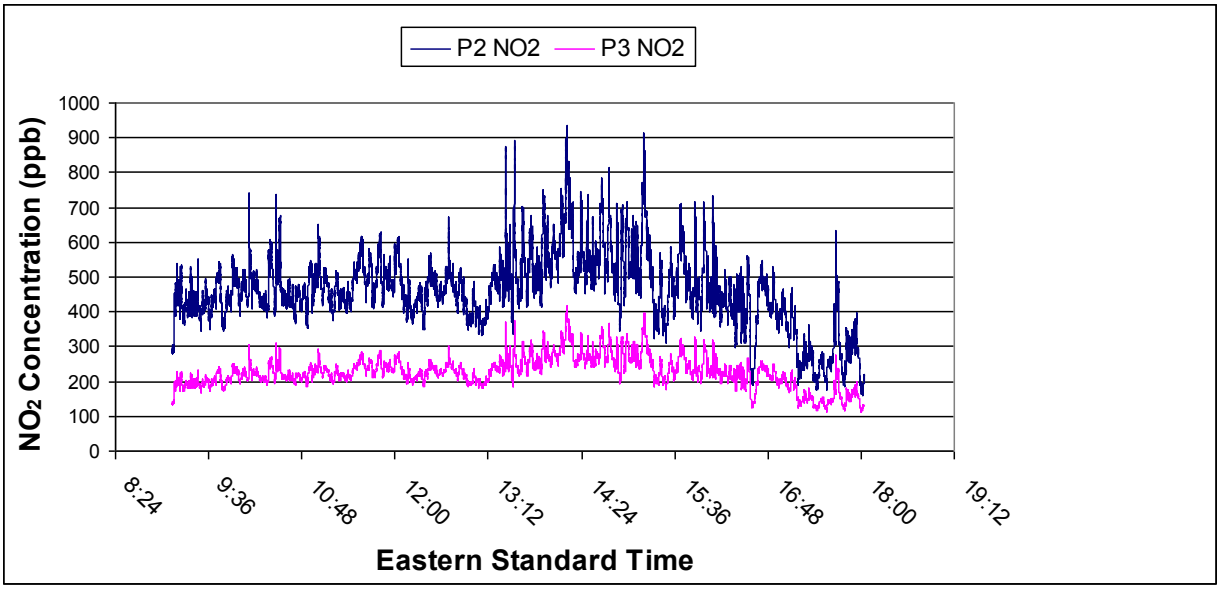

Figure 5.8. An Example of CAPS NO_2 concentrations measured before and after the DeNOx system.

CAPS data displayed in Figure 5.8 were measured at 1 Hz resolution and these two data sets have been time aligned to account for the spatial separation of these instruments within the AFP. These data clearly show the highly transient behaviour of the NO_2 signature within the AFP. It should be noted that the CM NOx analysers that were utilised for NO_2 concentration measurements that were reported in Section 5 were unable to resolve these rapidly changing NO_2 concentrations due to the slower response time of the CM instruments. The rapid response times of these CAPS instruments combined with their increased sensitivity (<1ppb) significantly improved the accuracy of NO_2 concentration measurements and hence, the accuracy of the calculated NO_2 removal efficiency of the DeNOx system.

Figure 5.9 shows an example of NO_2 removal efficiency calculated from the CAPS instruments

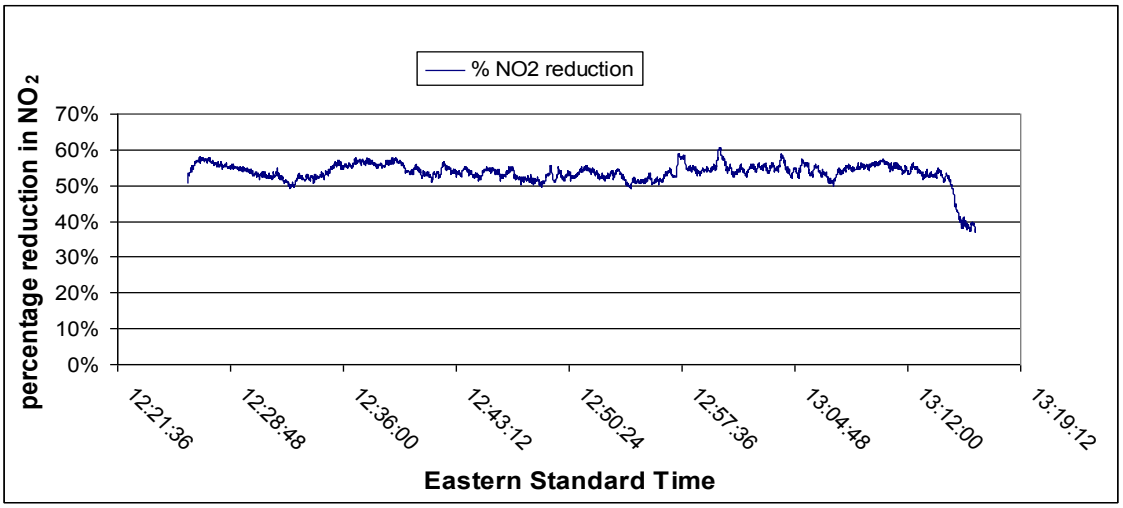

Figure 5.9. An Example of CAPS NO_2 removal efficiency data for the DeNOx system.

The average CAPS data shown in Figure 5.9 indicate that the NO_2 removal efficiency of the DeNOx system is of the order of 55%, a value that is consistent with the calculated NO_2 removal efficiencies based on CM measurements.

Some CAPS data sets have suggested that there is a reduction in removal efficiency of the DeNOx system with increased run time of the system. This artefact can be observed in Figure 5.10 with the removal efficiency progressively decreasing over the time period of these data.

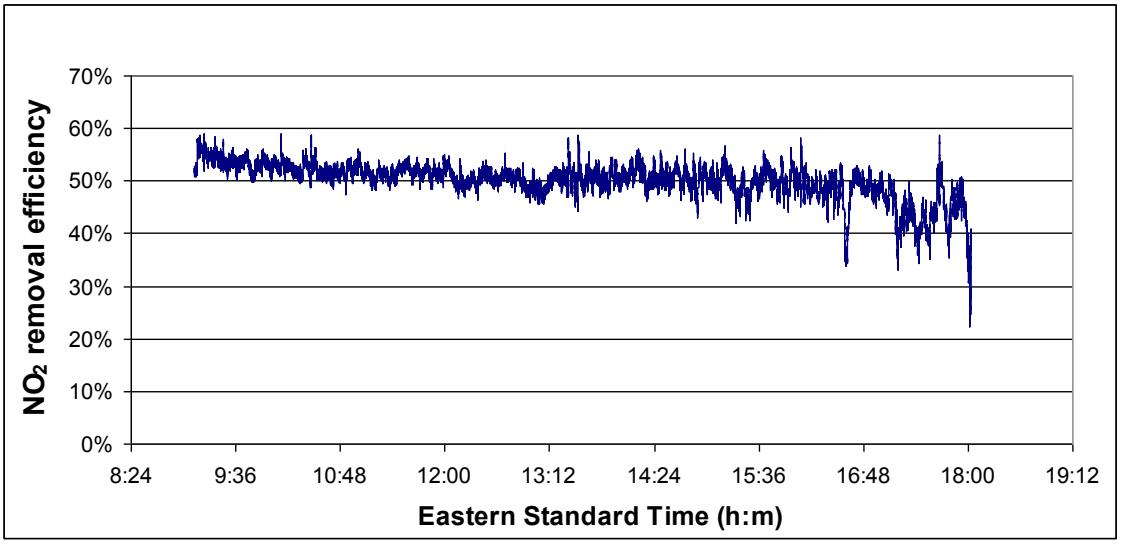

Figure 5.10. An Example of CAPS NO_2 removal efficiency data displaying reducing efficiency with respect to operation time.

As the CAPS instruments were received towards the end of this study this unusual behaviour shown in Figure 5.10 has not been fully investigated. As such, these finding should be considered speculative until further research has been completed. However, even if these findings are considered speculative, these data suggest that the NO_2 removal chemistry is complex.

The increased accuracy and response of the CAPS NO_2 measurements enabled the relationship between NO_2 removal efficiency and the upstream NO_2 concentration (called initial concentration in Figure 5.11) to be investigated. This relationship is displayed in Figure 5.11.

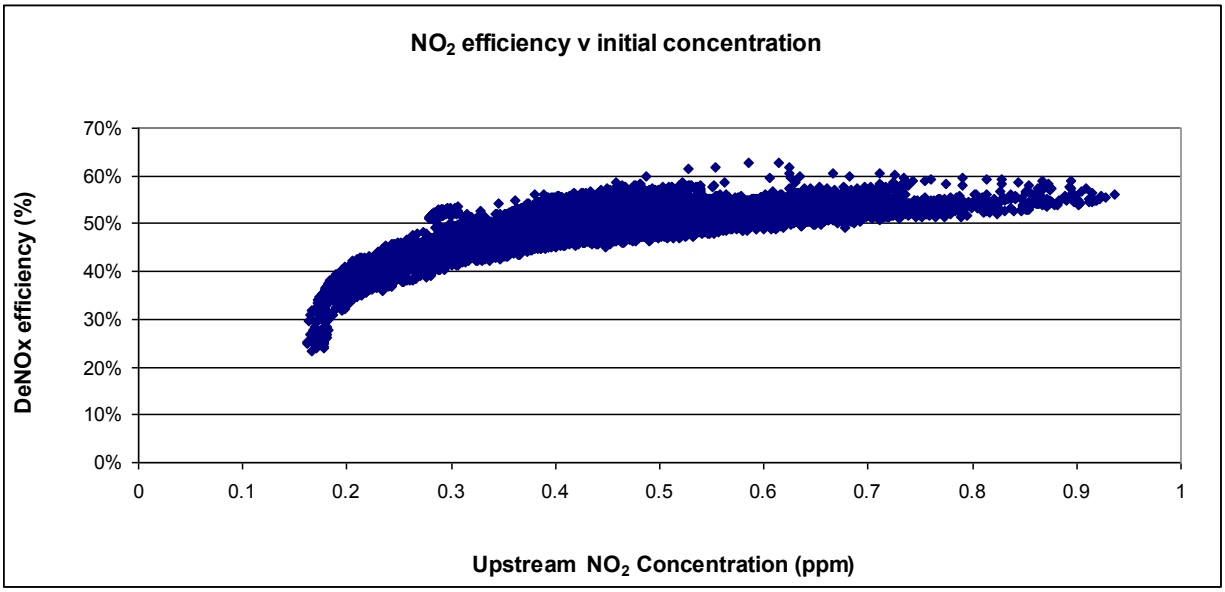

Figure 5.11. Dependence of NO_2 removal efficiency data with respect to initial NO_2 concentrations.

The data set displayed in Figure 5.11 exhibit a strong relationship between upstream NO_2 concentrations and NO_2 removal efficiency of the AFP DeNOx system. These data indicate that the removal efficiency is not linear with respect to NO_2 concentration and tends to reduce rapidly at concentrations of less than approximately 0.2ppm. These data suggest that a lower NO_2 removal efficiency limit may exist for the activated carbon used in the DeNOx and for the gas condition of the AFP. However, this hypothesis is speculative and thus more research if these findings are to be confirmed.

These data also indicate that the removal efficiency asymptotes to a constant value of approximately 55% as NO_2 concentration increases. These data provide further evidence that the NO_2 removal chemistry is complex and requires more research to fully investigate the kinetic relationship between NO_2 removal rates and NO_2 concentrations. It is likely that the sensitivity of the NO_2 removal efficiency to the upstream NO concentration would need to be included in any further studies.

5.8 Conclusion

The CAPS instrumentation provided the most accurate and reliable NO_2 removal efficiencies with NO_2 removal efficiency of 55%. At the time of writing this report a full study into the uncertainty of this instrument had not been completed. However, it is speculated that from the manufacturers quoted specifications, that define a NO_2 lower detection limit of less than 1ppb, in addition to published results, the uncertainty of these CAPS generated NO_2 concentration data would be 5% or less.

6 NO_2 AND NO REMOVAL EFFICIENCY MEASUREMENTS USING AN INTEGRATED SAMPLING TECHNIQUE.

As highlighted in Section 5, “Real time” CM determinations of the NO_2 and NO removal efficiency for the DeNOx system includes a large degree of uncertainty. These large uncertainties arise as a result of the compounding of smaller uncertainties that include instrumental uncertainties of the NOx analysers and gas dilution instrumentation, calibration uncertainties, uncertainties due to correction for spatial separation of the instruments as well as the uncertainty in the response times of these instruments. To improve the accuracy of the NO_2 and NO removal efficiency determinations using CM instrumentation, an integrated sampling approach was used. This approach utilised a synchronised timed filling of Teflon sample bags (SKC, USA). It is noted that the CAPS NO_2 analyser had not been acquired at the time of these measurements.

6.1 Overview of the NO and NO_2 Time Integrated Sampling Technique and Apparatus using CM analyses.

This sampling technique utilises the synchronised filling of Teflon sample bags to obtain a time integrated gas sample. The apparatus is shown below in Figure 6.1 and again in a schematic form in Figure 6.2.

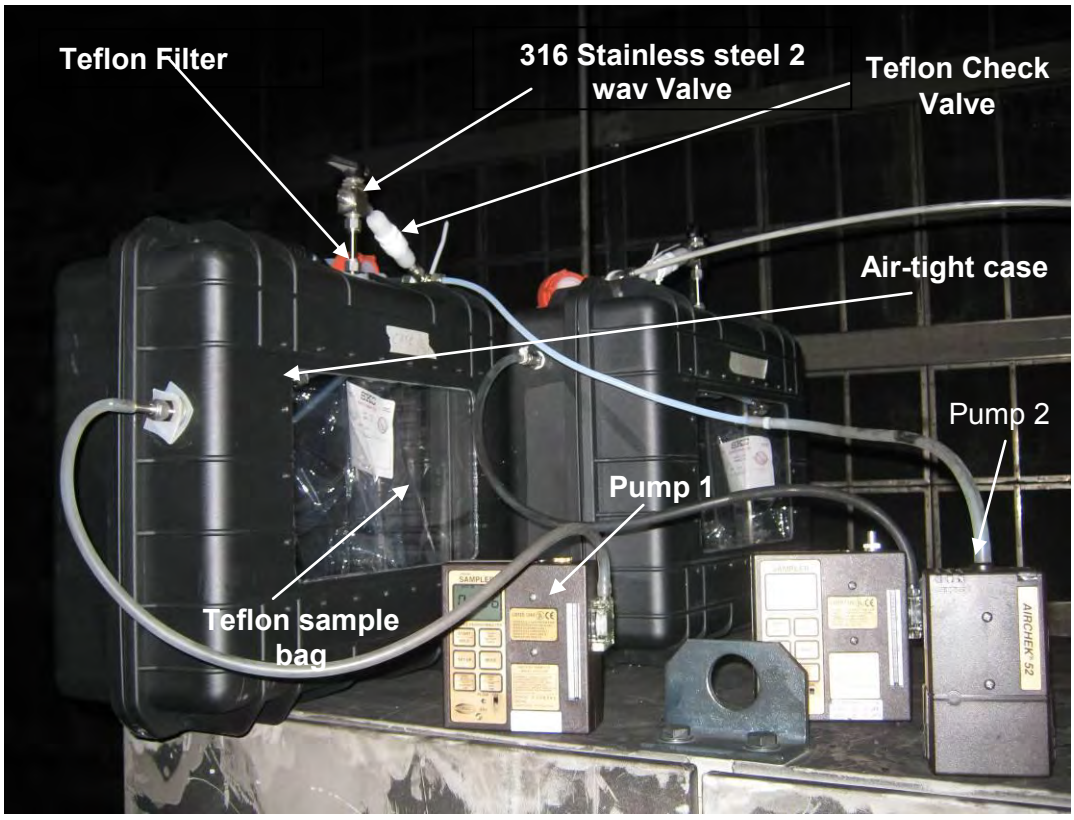

Figure 6.1. Apparatus used to collect integrated gas samples within the AFP. Two co-located samplers positioned at “P 3”.

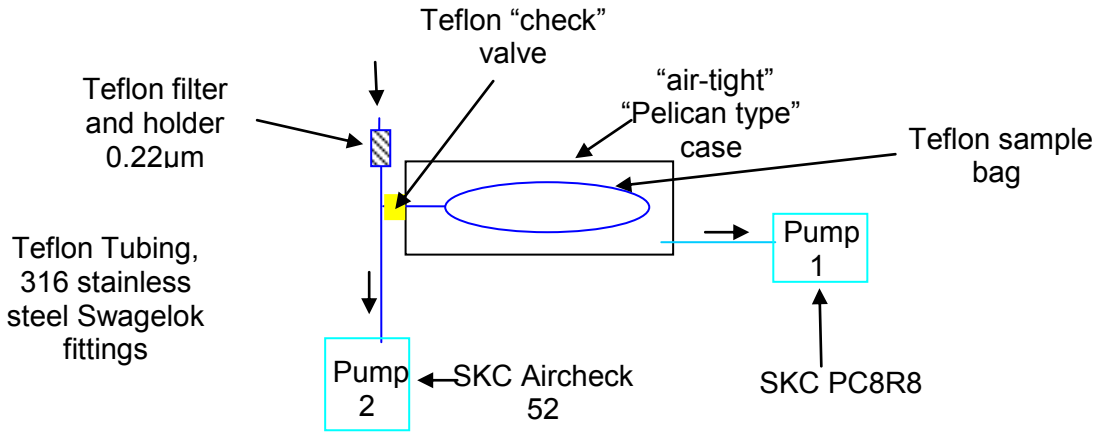

Figure 6.2. Schematic diagram of the apparatus used to collect integrated gas samples within the AFP.

To undertake the time integrated gas sampling measurements four identical sets of the sampling apparatus were used. The use of four samplers enabled the co-location of these samplers to validate the precision of this technique.

During normal operation of the air sampling apparatus, sample air was continuously drawn through the Teflon filter (0.22µm) and filter holder assembly, through the Teflon sample tubes and then past the inlet to the "check" valve by the action of "pump 2". "Pump 1" was programmed to commence sampling at a preset time and this pump exhausted air from the interface between the air-tight case and the Teflon sample bag. At a preset differential pressure that was common to all four samplers, the check valve located at the inlet to the Teflon bag opened enabling sample air to pass into each Teflon sample bag without direct pumping of the gas sample. After a predetermined time period pump 1 was programmed to stop sampling. Once pump 1 stopped operating the check valve automatically closed thereby sealing the bag to further air ingress. For each sampling apparatus set, pump 1 was co-ordinated to commence and stop sampling at common start times and operate for the same run periods. Thus each sample bag filled at the same rate and over the same time period.

NO and NOx analyses were completed using a single Thermo 42i CM analyser operating in switching mode and calibrated with a NATA certified calibration gas (Coregas) directly before and directly after a measurement series. By utilising a single CM NOx analyser for gas analyses, uncertainties were reduced. Additionally, since gas samples were collected over 12 minute periods uncertainties associated with time alignment errors were reduced.

Before deployment of these samplers:

1 The reproducibility of this technique was determined by repeated filling of the sample bag with a constant concentration of NO and NO_2 (Coregas, NATA certified) and then analysing the gas sample. Repeatability was found to be similar to the repeatability of the NOx analyser alone.

2 The long term stability of the NOx gas when contained in the Teflon sample bag was assessed. The sample bags were filled with a NOx gas sample and stored for 12 hours after which the NO and NOx concentrations were re-measured. The reproducibility of the NO and NO_2 concentrations were measured to be within the uncertainty band of the NOx analyser alone.

3 Sample bag flushing and sample filling procedures were developed.

Using the technique described in this section, the spatial homogeneity of the NOx concentration signature before and after the DeNOx system was examined by sampling at spatially different locations. During these measurements, the variation of NO and NOx concentrations of spatially separated measurements were within the precision of this technique ~5%. In addition, the precision of the technique was assessed by comparing the results of co-located samplers. Summaries of the results from these measurements are shown in Table 3 while a summary of the measurements used to validate this technique and assess the precision are detailed in Tables 6.1 and 6.2.

Table 6.1. NO and NO_2 Removal Efficiency Results - Integrated Gas Sampling Technique.

Efficiency Measurements											
Date	Position	Time	Fan speed*	NOx**	NO**	NO_2**	NOx**	NO**	NO_2**	NO_2 Removal (%)	NO Removal (%)
19-May	A		35	3.38	3.17	0.22	3.01	2.91	0.09	57.4%	8.0%
24-May	A		35	2.49	2.24	0.25	2.23	2.09	0.14	44.6%	6.6%
26-May	A	5:30pm	35	3.21	2.88	0.33	2.67	2.53	0.14	56.3%	12.3%
26-May	A	6:00pm	35	4.11	3.74	0.37	3.22	3.05	0.18	53.0%	18.4%
26-May	A	6:30pm	35	2.59	2.30	0.29	2.19	2.05	0.13	53.1%	10.9%
30-May	A	4:30pm	35	3.55	3.24	0.31	2.87	2.73	0.14	55.4%	15.9%
30-May	A	5:00pm	35	1.89	1.68	0.20	1.64	1.55	0.08	58.9%	7.7%
30-May	A	5:20pm	50	2.20	1.95	0.25	1.96	1.86	0.10	59.1%	4.8%
30-May	A	5:40pm	50	2.87	2.56	0.30	2.30	2.17	0.13	57.1%	15.3%
30-May	A	6:00pm	70	3.04	2.70	0.34	2.72	2.57	0.15	56.3%	4.6%
1-Jun	A	11:30am	40	4.04	3.66	0.38	3.23	3.04	0.19	51.5%	16.8%
1-Jun	A	11:50am	60	4.27	3.86	0.41	3.45	3.27	0.19	54.4%	15.4%
1-Jun	A	12:12pm	80	4.17	3.77	0.41	3.58	3.39	0.19	54.0%	9.9%
1-Jun	A	12:30pm	90	4.65	4.24	0.41	3.86	3.68	0.17	57.9%	13.0%
1-Jun	A	3:00pm	70	4.78	4.25	0.53	3.82	3.61	0.21	61.0%	15.1%
28-Jun	A	12:00pm	40	4.07	3.64	0.42	3.22	3.01	0.20	52.6%	17.3%
28-Jun	A	4:30pm	40	2.75	2.41	0.34	2.42	2.25	0.17	48.6%	6.9%
28-Jun	A	5:00pm	40	3.82	3.45	0.38	3.17	3.00	0.17	54.8%	13.0%
30-Jun	A	4:30pm	40	2.90	2.68	0.22	2.47	2.37	0.10	55.0%	11.6%
30-Jun	A	6:00pm	40	2.09	1.93	0.16	1.91	1.83	0.07	53.0%	5.1%
30-Jun	A	7:30pm	40	2.00	1.87	0.13	1.83	1.77	0.06	57.3%	5.1%
30-Jun	A	8:30pm	40	2.86	2.59	0.28	2.44	2.34	0.11	61.8%	9.7%
1-Jul	A		40	6.58	5.90	0.68	4.80	4.53	0.27	60.0%	23.2%
							Average			55%	12%
							Standard Deviation			4%	5%
					Final Result Range			Min.	Max		
					2 x standard deviation			47.5%	63.3%		

* As percentage of the maximum fan speed. ** Gas concentration (ppm)

Position Key A - Adjacent P 2

Table 6.2. NO and NO_2 Validation Results - Integrated Gas Sampling Technique.

Validation Measurements											
Date	Position	Time	Fan speed*	NOx**	NO**	NO_2**	NOx**	NO**	NO_2**	NO_2 Removal (%)	NO Removal (%)
31-May	B	1:30pm	35	3.79	3.38	0.41	3.71	3.34	0.38	8.2%	1.2%
31-May	B	3:00pm	35	3.94	3.52	0.42	3.90	3.49	0.41	3.9%	0.7%
31-May	C	3:30pm	35	4.00	3.55	0.45	3.89	3.44	0.45	-0.7%	3.2%
31-May	D	4:00pm	35	2.96	2.78	0.19	2.97	2.79	0.18	1.6%	-0.2%
31-May	E	4:30pm	35	3.96	3.55	0.41	3.99	3.58	0.41	-0.9%	-0.8%
31-May	E	4:40pm	80	2.56	2.22	0.33	2.60	2.29	0.31	6.6%	-2.9%
1-Jun	F	4:30pm	35	3.59	3.23	0.35	3.54	3.21	0.33	7.2%	0.7%
28-Jun	B	4:30pm	40	2.75	2.41	0.33	2.76	2.41	0.34	-2.4%	0.0%
28-Jun	G	4:30pm	40	2.40	2.23	0.17	2.44	2.27	0.17	1.1%	-1.9%
28-Jun	B	5:00pm	40	3.84	3.46	0.38	3.81	3.43	0.38	-0.8%	1.1%
28-Jun	G	5:00pm	40	3.13	2.97	0.16	3.22	3.03	0.18	-17.1%	-2.1%
30-Jun	B	4:30pm	40	2.89	2.68	0.21	2.91	2.68	0.22	-8.0%	0.0%
30-Jun	G	4:30pm	40	2.49	2.40	0.09	2.45	2.35	0.10	-5.0%	2.0%
30-Jun	G	6:30pm	40	1.90	1.83	0.07	1.92	1.84	0.08	-9.3%	-0.3%
30-Jun	H	7:30pm	40	1.99	1.86	0.13	2.00	1.87	0.13	1.3%	-0.5%
30-Jun	I	8:30pm	40	2.92	2.65	0.28	2.80	2.53	0.27	2.0%	4.3%
30-Jun	J	8:30pm	40	2.40	2.32	0.08	2.48	2.35	0.13	-51.6%	-1.4%
1-Jul	K		40	6.66	5.99	0.67	6.50	5.82	0.68	-0.6%	2.9%
							Average			-3.6%	0.3%
							St Dev			13.5%	1.9%

Position Key

B - Adjacent P 2 C - Opposite and after ESP D - Front and back of DeNOx
E - P 2 and P 4 F - P 1 and P 2 G - Adjacent P 3
H - Opposite ESP I - Mid To Top ESP J - Side of Carbon boxes to P 3
K - Increasing radius outside DeNOx

* As percentage of the maximum fan speed.
** Gas concentration (ppm)

6.2 NO and NO_2 removal efficiency and DeNOx fan speed.

The impact of DeNOx fan speed upon NO and NO_2 removal efficiencies was also investigated while undertaking time integrated gas sampling measurements. For these measurements the DeNOx fan speed was systematically varied from 35% to 100% of the maximum available fan speed and the removal efficiency of each target gas measured. These data are shown in figure 6.3.

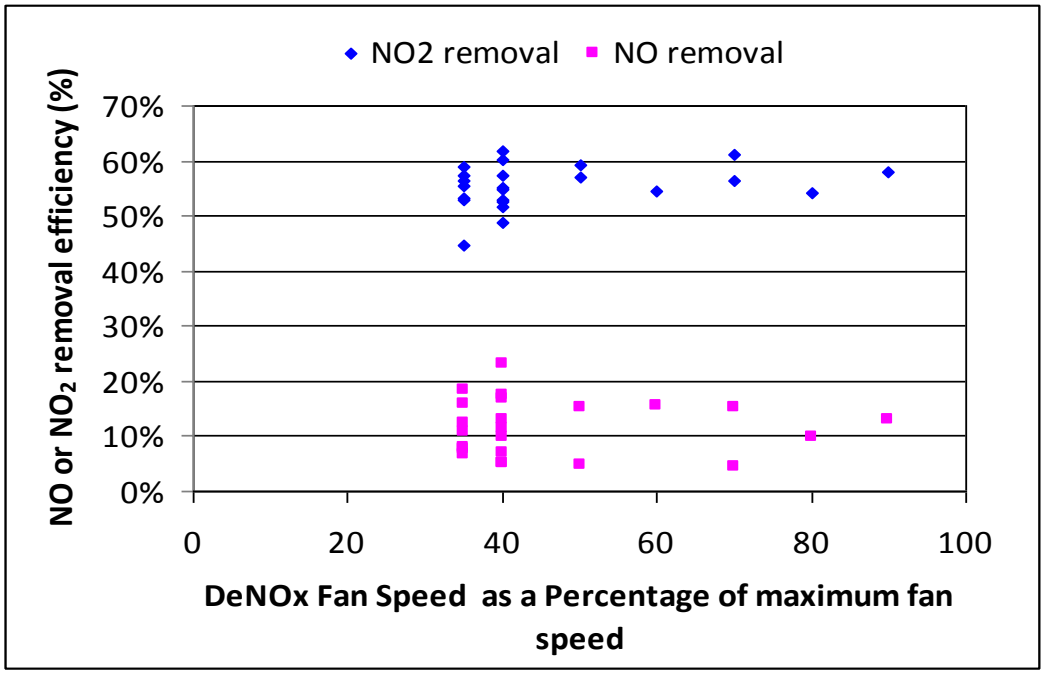

Figure 6.3. NO and NO_2 removal efficiency as a function of DeNOx fan speed.

Data displayed in Figure 6.3 describe the NO and NO_2 removal efficiencies as a function of the operating speed of the fans. Both for NO and NO_2, these data show a nearly constant removal efficiency. This was an unexpected result and suggests that the DeNOx system could be operated at larger flow rates without a loss in removal efficiency. Further research is required before a more thorough and detailed understanding of this artefact is acquired.

6.3 Conclusion.

The integrated gas sampling technique has provided highly reproducible NO and NO_2 removal efficiency results with a NO_2 removal of 55% and with a precision of 8% (2 standard deviations) and a NO removal efficiency of 12% with a precision of 10% (2 standard deviations).

7 INVESTIGATION OF THE NO AND NO_2 REMOVAL EFFICIENCY OF THE ACTIVATED CARBON USE WITHIN DeNOx SYSTEM.

Activated carbon has been successfully utilised in a number of industries for the mitigation of NO_2. As such, the chemical reactions of NO_2 that occur at the surface of activated carbon are reasonably well understood (Teng and Suuberg, 1993; Kang et al, 2009; Lopez, et al, 2007; Zawadzki, Wisniewski, Skowronska, 2003; Guo et al, 2001). Additionally, activated carbon has previously been used as a catalytic NO_2 to NO converter for some commercial CM NOx analysers such as the Rosemount Analytical NGA Wet Chemiluminescence Detection Analyzer Module. The response of carbon based NO_2 converters has also been examined previously (Pitts, 1974).

The measurements reported in Sections 5 and 6 of this report, revealed that the NO_2 removal efficiency of the DeNOx system was less than the removal efficiencies that have been reported in the open literature for activated carbon. Correspondingly, a research program was initiated to investigate the NO_2 removal efficiencies of activated carbon alone. To complete this work CSIRO constructed a Activated Carbon Test Apparatus (ACTA) that allowed the NO and NO_2 removal efficiency of the activated carbon to be measured under controlled conditions and independently of the DeNOx system.

7.1 NO and NO_2 removal "Test" Apparatus.

The NO and NO_2 removal efficiencies of activated carbon as well as the NO and NO_2 removal efficiencies of individual filled boxes of "used" activated carbon from the DeNOx system were measured. A schematic diagram of the ACTA is shown in Figure 7.1.

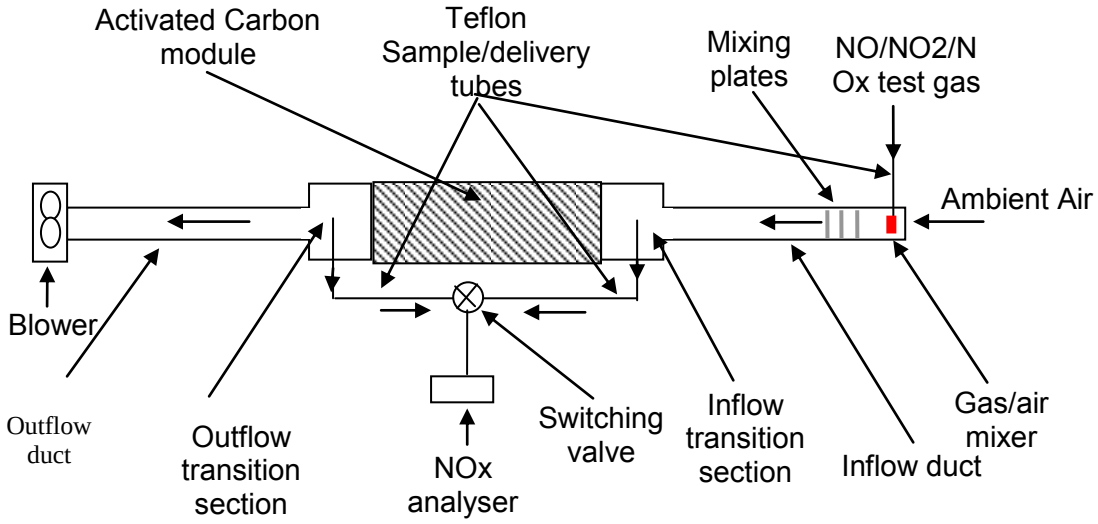

Figure 7.1. Schematic diagram of the ACTA.

The ACTA shown in Figure 7.1 was designed around two sections of ductwork. One section of this ductwork was clamped over the inlet of an activated carbon module and this section presented the module with a well mixed and uniform gas sample. The second section was clamped to the outlet of the module and provided an area of laminar gas flow just after the module. These areas of laminar flow before and after the module were used as sampling planes for NOx measurements. The outlet from ductwork after the module was connected to the blower. At the air inlet, ambient air was drawn into the pipe and this air was mixed with

the test gas (Coregas, NATA certified NO, NO_2 or NOx mixture) through a gas mixing system. The test gas was delivered in a diluted form and at a constant flow rate using a mass flow controller. The diluted test gas then passed through three mixing plates that produced localised gas turbulence and increased mixing of the test gas with ambient dilution air. A transition section was placed between the test gas delivery tube and the inlet of the activated carbon module that facilitated further mixing of the gas and allowed the CM NOx analyser to sample the test gas at several points across the inlet area of the activated carbon module. Initial validation measurements of the ACTA showed that the inlet gas mixture that was presented to the inlet of the activated carbon module was homogeneous in gas concentration across the inlet plane.

The CM NOx analyser was connected to the inlet and outlet sections of the test apparatus stream by a 3-way ball valve. NO and NO_2 removal efficiencies were calculate by the difference in gas concentration between the inlet and outlet sample streams. Gas velocities were generally selected so that the velocity through the test module simulated the conditions within the DeNOx system.

Figure 7.2 shows the ACTA while Figure 7.3 shows the sampling section but at increased resolution.

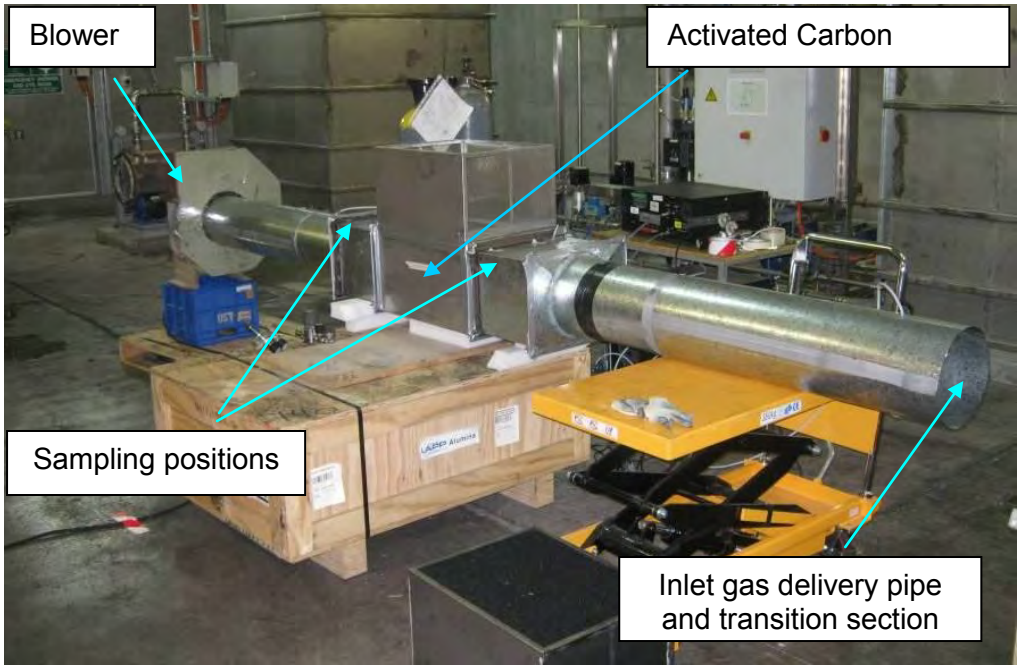

Figure 7.2. The ACTA installed within the AFP.

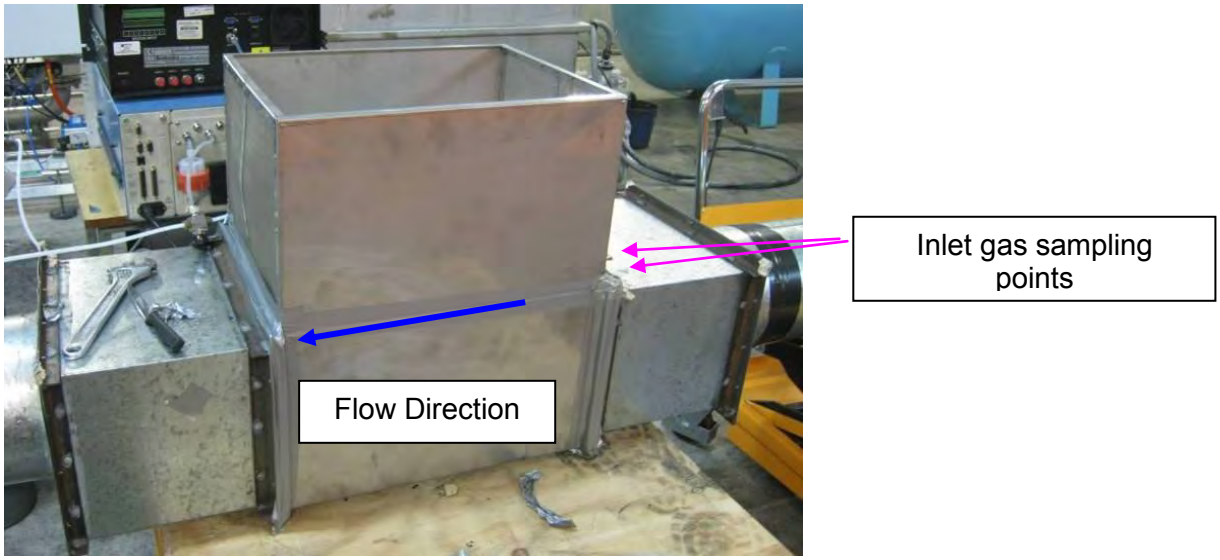

Figure 7.3. The inlet and outlet sampling sections of the ACTA.

The inlet section to the ACTA is shown in Figure 7.3 where two of the sampling points across the inlet plane can be observed. These sampling points consisted of holes in the steel sheeting through which Teflon tubing penetrated to a predetermined position. The tubing was sealed in place with adhesive tape and the unused holes were sealed with adhesive tape when not used. Similar outlet sampling points were located across the outlet sampling plane.

The ACTA was used to undertake a wide range of measurements including:

- NO ands NO_2 removal efficiency measurements of "new"or unused activated carbon
- NO ands NO_2 removal efficiency measurements of previously used activated carbon (activated carbon modules carefully removed from the activated carbon assembly of the DeNOx system and installed into the ACTA)
- NO and NO_2 removal efficiency measurements of used activated carbon while in the normal operating position and just after normal operation of the DeNOx system
- Measurements directed towards understanding the chemistry of the NO and NO_2 removal processes.

Figure 7.4 shows the carbon test apparatus installed across the DeNOx system. Only the inlet of the ACTA is shown. The ACTA outlet and blower were located on the opposite side of the corresponding activated carbon filled module.

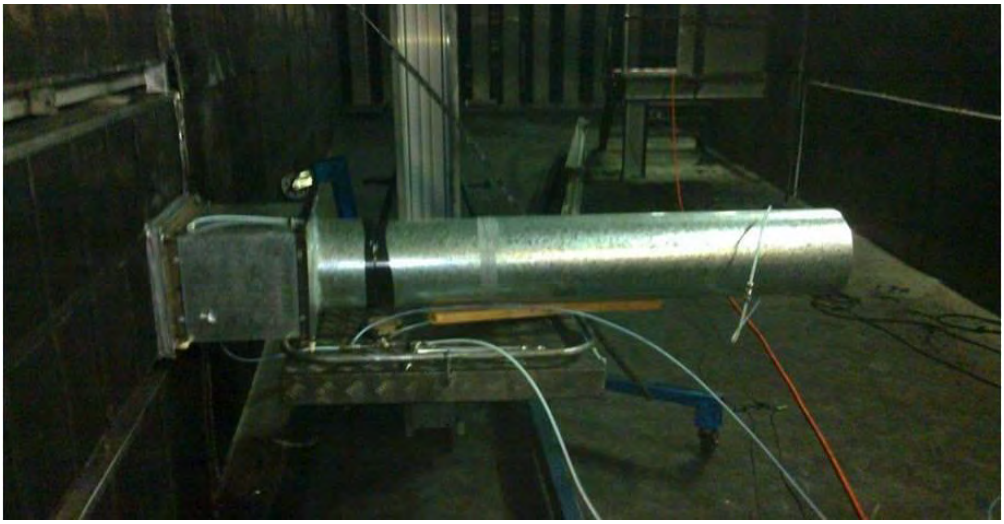

Figure 7.4. The inlet sampling section interfaced to the inlet side of the ACTA when installed across the DeNOx support structure.

The NO and NO_2 removal efficiency measurements undertaken with the ACTA are summarised in Tables 7.1.

Table 7.1. Summary Of NO and NO_2 Removal Efficiencies – ACTA.

Date	Carbon description	Input gas	Flow through box (L/s)	NOx before	NO before	NO_2	NOx after	NO after	NO_2	NO_2 %	NO %	NO_2=1, NO=0	New=1, Used=0	NO_2 new	NO_2 used	NO new	NO used	
20-Apr	New	16ppm NO_2	92			0.216			0.015	92.9%		1	1	92.9%				
2-May	New	101.1ppm NOx, 96.9 NO	92	1.138	1.031	0.106	0.499	0.486	0.014	87.1%	52.9%	0	1			52.9%		
10-May	New - NO input	101.1ppm NOx, 96.9 NO	71	1.421	1.287	0.134	0.463	0.449	0.014	89.3%	65.1%	0	1			65.1%		
	New - NO2 input	16ppm NO_2	71	0.231	0.000	0.231	0.004	0.004	0.000	99.9%		1	1	99.9%				
	New - NO input	101.1ppm NOx, 96.9 NO	37	1.498	1.368	0.131	0.523	0.510	0.013	90.0%	62.7%	0	1			62.7%		
	New - NO2 input	16ppm NO_2	37	0.247	0.001	0.246	0.003	0.003	0.001	99.7%	-98.8%	1	1	99.7%				
	New - NO input	101.1ppm NOx, 96.9 NO	38	1.557	1.410	0.147	0.537	0.520	0.017	88.7%	63.1%	0	1			63.1%		
	New - NO2 input	16ppm NO_2	38	0.277	0.025	0.253	0.013	0.012	0.001	99.6%	51.8%	1	1	99.6%				
	New - NO input	101.1ppm NOx, 96.9 NO	19	2.380	2.160	0.220	0.429	0.417	0.012	94.5%	80.7%	0	1			80.7%		
	New - NO2 input	16ppm NO_2	19	0.447	0.014	0.433	0.008	0.006	0.002	99.6%	55.8%	1	1	99.6%				
7-Jun	Test rig in DeNOx	1600ppm NO	50	4.718	4.662	0.056	3.011	2.980	0.031	44.4%	36.1%	0	0				36.1%	
	Test rig in DeNOx	~100ppm NO_2	50	0.463	0.209	0.254	0.315	0.274	0.041	83.9%	-31.0%	1	0		83.9%			
	Test rig in DeNOx	~100ppm NO_2	50	0.463	0.207	0.256	0.313	0.277	0.036	85.8%	-33.8%	1	0		85.8%			
	Test rig in DeNOx	~100ppm NO_2	50	0.352	0.079	0.273	0.179	0.143	0.036	87.0%	-81.8%	1	0		87.0%			
8-Jun	Box extracted 7-6 and flushed overnight	~100ppm NO_2	50	0.283	0.127	0.157	0.138	0.131	0.007	95.7%	-3.8%	1	0		95.7%			
	Box extracted 7-6 and flushed overnight	~100ppm NO_2	50	0.257	0.075	0.183	0.123	0.113	0.010	94.6%	-51.0%	1	0		94.6%			
	Box extracted 7-6 and flushed overnight	~100ppm NO_2	50	0.220	0.045	0.175	0.092	0.079	0.013	92.5%	-75.7%	1	0		92.5%			
	Box extracted 7-6 and flushed overnight	1600ppm NO	50	4.198	4.084	0.114	3.099	3.014	0.085	25.8%	26.2%	0	0				26.2%	
	Box extracted 7-6 and wrapped in bag	~100ppm NO_2	50	0.269	0.101	0.168	0.174	0.132	0.043	74.7%	-29.9%	1	0		74.7%			
	Box extracted 7-6 and wrapped in bag	~100ppm NO_2	50	0.270	0.103	0.167	0.175	0.130	0.045	72.9%	-26.3%	1	0		72.9%			

9-Jun	Box extracted 7-6 and wrapped in bag	~100ppm NO_2	50	0.428	0.116	0.312	0.251	0.147	0.105	66.4%	-26.1%	1	0		66.4%			
	Box extracted 7-6 and wrapped in bag	~100ppm NO_2	50	0.455	0.144	0.311	0.271	0.173	0.098	68.5%	-20.4%	1	0		68.5%			
	Box extracted 7-6 and wrapped in bag	~100ppm NO_2	50	0.448	0.127	0.321	0.269	0.166	0.103	67.8%	-30.3%	1	0		67.8%			
4-Jul	New box filled 4-7	900ppm NO_2	50	1.831	0.089	1.742	0.084	0.076	0.009	99.5%	15.0%	1	1	99.5%				
	New box filled 4-7	900ppm NO_2	50	1.808	0.048	1.760	0.087	0.080	0.007	99.6%	-65.2%	1	1	99.6%				
	New box filled 4-7	900ppm NO_2	50	1.811	0.057	1.754	0.106	0.097	0.010	99.4%	-70.2%	1	1	99.4%				
	New box filled 4-7	900ppm NO_2	50	0.929	0.051	0.878	0.077	0.069	0.009	99.0%	-35.3%	1	1	99.0%				
	New box filled 4-7	900ppm NO_2	50	0.923	0.039	0.884	0.091	0.086	0.004	99.5%	-119.3%	1	1	99.5%				
	New box filled 4-7	900ppm NO_2	50	0.966	0.089	0.877	0.106	0.098	0.008	99.1%	-10.7%	1	1	99.1%				
6-Jul	New box filled 4-7	900ppm NO_2	50	1.394	0.076	1.318	0.093	0.097	-0.004	100.3%	-28.0%	1	1	100.3%				
	New box filled 4-7	900ppm NO_2	50	1.452	0.046	1.406	0.121	0.126	-0.005	100.3%	-173.2%	1	1	100.3%				
	New box filled 4-7	900ppm NO_2	50	1.466	0.057	1.408	0.161	0.169	-0.008	100.6%	-195.6%	1	1	100.6%				
	New box filled 4-7	900ppm NO_2	50	1.476	0.062	1.414	0.163	0.168	-0.005	100.3%	-169.9%	1	1	100.3%				
	New box filled 4-7	900ppm NO_2	50	1.477	0.055	1.422	0.174	0.173	0.001	99.9%	-214.8%	1	1	99.9%				
	New box filled 4-7	900ppm NO_2	50	0.640	0.042	0.597	0.090	0.093	-0.003	100.5%	-119.5%	1	1	100.5%				
	New box filled 4-7	900ppm NO_2	50	0.631	0.041	0.590	0.090	0.091	-0.001	100.2%	-122.1%	1	1	100.2%				
	New box filled 4-7	900ppm NO_2	50	0.632	0.048	0.583	0.118	0.128	-0.010	101.7%	-164.4%	1	1	101.7%				
	New box filled 4-7	900ppm NO_2	50	0.716	0.109	0.607	0.117	0.118	-0.002	100.2%	-8.8%	1	1	100.2%				
	New box filled 4-7	900ppm NO_2	50	0.643	0.045	0.598	0.109	0.117	-0.007	101.2%	-157.4%	1	1	101.2%				
	New box filled 4-7	900ppm NO_2through conv	50	1.804	1.731	0.074	0.855	0.876	-0.021	128.4%	49.4%	0	1			49.4%		
	New box filled 4-7	900ppm NO_2through conv	50	1.813	1.521	0.292	0.760	0.798	-0.038	112.8%	47.5%	0	1			47.5%		
	New box filled 4-7	900ppm NO_2through conv	50	1.819	1.368	0.451	0.696	0.719	-0.023	105.2%	47.4%	0	1			47.4%		
	New box filled 4-7	900ppm NO_2through conv	50	1.848	1.194	0.654	0.607	0.629	-0.022	103.4%	47.4%	0	1			47.4%		
	New box filled 4-7	900ppm NO_2through conv	50	1.807	1.008	0.798	0.570	0.587	-0.017	102.1%	41.8%	0	1			41.8%		
	Top of 2 boxes removed after AFP use that day	900ppm NO_2	50	1.418	0.082	1.337	0.507	0.245	0.262	80.4%	-201.1%	1	0		80.4%			

	Top of 2 boxes removed after AFP use that day	900ppm NO_2	50	1.441	0.071	1.370	0.547	0.265	0.281	79.5%	-274.7%	1	0		79.5%			
	Top of 2 boxes removed after AFP use that day	900ppm NO_2	50	1.457	0.076	1.381	0.611	0.311	0.300	78.3%	-311.6%	1	0		78.3%			
	Top of 2 boxes removed after AFP use that day	900ppm NO_2	50	1.494	0.092	1.401	0.671	0.334	0.337	75.9%	-261.1%	1	0		75.9%			
	Top of 2 boxes removed after AFP use that day	900ppm NO_2	50	1.475	0.089	1.386	0.700	0.365	0.335	75.8%	-310.0%	1	0		75.8%			
	Top of 2 boxes removed after AFP use that day	900ppm NO_2	50	0.769	0.087	0.682	0.461	0.334	0.127	81.3%	-283.2%	1	0		81.3%			
	Top of 2 boxes removed after AFP use that day	900ppm NO_2	50	0.790	0.120	0.670	0.479	0.358	0.121	81.9%	-198.1%	1	0		81.9%			
	Top of 2 boxes removed after AFP use that day	900ppm NO_2	50	0.792	0.097	0.695	0.493	0.368	0.125	82.0%	-279.8%	1	0		82.0%			
	Top of 2 boxes removed after AFP use that day	900ppm NO_2	50	0.791	0.100	0.691	0.514	0.388	0.126	81.8%	-290.3%	1	0		81.8%			
	Top of 2 boxes removed after AFP use that day	900ppm NO_2	50	0.782	0.084	0.697	0.516	0.385	0.132	81.1%	-356.1%	1	0		81.1%			
7-Jul	Top of 2 boxes, removed 6-7, very high NO2	900ppm NO_2	50	17.054	0.138	16.916	4.843	2.008	2.835	83.2%	-1355.1%	1	0		83.2%			
8-Jul	Bottom of 2 boxes removed 6-7	900ppm NO_2	50	1.297	0.011	1.286	0.192	0.105	0.087	93.2%	-873.7%	1	0		93.2%			
	Bottom of 2 boxes removed 6-7	900ppm NO_2	50	1.311	0.015	1.296	0.246	0.142	0.104	92.0%	-871.7%	1	0		92.0%			
	Bottom of 2 boxes removed 6-7	900ppm NO_2	50	1.309	0.008	1.301	0.317	0.193	0.124	90.5%	-2296.9%	1	0		90.5%			
	Bottom of 2 boxes removed 6-7	900ppm NO_2	50	1.309	0.003	1.306	0.345	0.217	0.128	90.2%	-6798.9%	1	0		90.2%			
	Bottom of 2 boxes removed 6-7	900ppm NO_2	50	1.317	0.006	1.310	0.380	0.251	0.129	90.2%	-3939.8%	1	0		90.2%			
	Bottom of 2 boxes removed 6-7	900ppm NO_2	50	0.571	0.009	0.562	0.317	0.222	0.095	83.1%	-2278.8%	1	0		83.1%			
	Bottom of 2 boxes removed 6-7	900ppm NO_2	50	0.578	0.016	0.562	0.312	0.218	0.094	83.2%	-1250.1%	1	0		83.2%			

	Bottom of 2 boxes removed 6-7	900ppm NO_2	50	0.581	0.017	0.564	0.311	0.220	0.091	83.9%	-1198.5%	1	0		83.9%			
	Bottom of 2 boxes removed 6-7	900ppm NO_2	50	0.582	0.017	0.565	0.307	0.221	0.087	84.7%	-1191.3%	1	0		84.7%			
	Bottom of 2 boxes removed 6-7	900ppm NO_2	50	0.570	0.010	0.559	0.306	0.220	0.086	84.6%	-2090.1%	1	0		84.6%			
	Same box, with baffle inserted	900ppm NO_2	50	1.630	0.145	1.484	0.462	0.430	0.032	97.9%	-195.6%	1	0		97.9%			
	Same box, with baffle inserted	900ppm NO_2	50	1.672	0.132	1.540	0.431	0.418	0.013	99.1%	-217.5%	1	0		99.1%			
	Same box, with baffle inserted	900ppm NO_2	50	1.594	0.064	1.529	0.455	0.425	0.030	98.1%	-561.0%	1	0		98.1%			
	Same box, with baffle inserted	900ppm NO_2	50	1.632	0.086	1.545	0.472	0.463	0.009	99.4%	-436.2%	1	0		99.4%			
	Same box, with baffle inserted	900ppm NO_2	50	1.607	0.075	1.532	0.492	0.474	0.018	98.8%	-532.1%	1	0		98.8%			
	Same box, with baffle inserted	900ppm NO_2	50	0.711	0.067	0.644	0.500	0.426	0.019	97.0%	-533.4%	1	0		97.0%			
	Same box, with baffle inserted	900ppm NO_2	50	0.772	0.126	0.646	0.500	0.478	0.021	96.7%	-280.9%	1	0		96.7%			
	Same box, with baffle inserted	900ppm NO_2	50	0.847	0.178	0.669	0.462	0.467	-0.005	100.8%	-162.1%	1	0		100.8%			
	Same box, with baffle inserted	900ppm NO_2	50	0.746	0.095	0.651	0.434	0.415	0.019	97.0%	-335.6%	1	0		97.0%			
	Same box, with baffle inserted	900ppm NO_2	50	0.765	0.126	0.639	0.488	0.471	0.017	97.3%	-274.6%	1	0		97.3%			
														NO_2 **new**	NO_2 **used**	**NO new**	**NO used**	**NO_2 baffle**
											Average			99.7%	82.7%	55.8%	31.2%	98.2%
											Standard Deviation			1.7%	7.6%	11.9%	7.0%	1.3%

7.2 Comparison of ACTA based NO and NO_2 removal efficiencies of activated carbon and DeNOx removal efficiencies.

Depending upon the type of measurement the activated carbon modules were either fully filled with new carbon, "topped up" with "used" carbon or used in an "as removed" condition. The activated carbon sample was then challenged with a range of concentrations of NO and NO_2. The "new" activated carbon was a fresh sample of carbon from the original bulk activated carbon sample. The "used" activated carbon was from modules that had been carefully extracted from the DeNOx system. NO and NO_2 gases were administered both separately and also as a mixture of these two gases over the course of this study. These results are summarised below in Table 7.2 and Table 7.3.

Table 7.2. NO_2 Removal Efficiency Results – ACTA based measurements.

	NO_2 removal efficiency new activated Carbon	NO_2 removal efficiency "used" activated Carbon	Overall NO_2 removal efficiency of DeNOx System
Average efficiency	>99%	83%	55%
Standard Deviation	2%	8%	4%

Table 7.3. NO Removal Efficiency Results – ACTA based measurements.

	NO removal efficiency new activated Carbon	NO removal efficiency "used" activated Carbon	Overall NO removal efficiency of DeNOx System
Average efficiency	56%	31%	12%
Standard Deviation	12%	7%	5%

Measurements undertaken on the ACTA are summarised in Table 7.2 and Table 7.3. These data show a significantly larger NO_2 removal efficiency for both the "new" activated carbon (>99%) and used activated carbon (>83%) when compared to corresponding measurements for the DeNOx system. NO removal efficiencies were also significantly greater for the ACTA and this is reflected in the NO efficiency results shown in Table 7.3.

7.3. Origins of the Smaller NOx removal efficiencies of the DeNOx system compared to the ACTA measurements.

It was observed that the activated carbon modules installed within the DeNOx system were not fully filled with activated carbon and this suggested that a large amount of the air passing through the module was passing over the top of the activated carbon. Figure 7.5 shows two boxes that had been carefully withdrawn form the DeNOx system.

Figure 7.5. Examples of Activated Carbon Modules that had been removed from the DeNOx system.

The module towards the left in Figure 7.5 was positioned underneath the rightmost module when these two modules were packed within the DeNOx system. This vertical stacking of pairs of modules allowed the lower module to be sealed by “close fit” and weight of the module stacked above. The upper module of the stacked pair of modules was sealed by a sheet of stainless steel that was lightly held in place by spring fittings. The uppermost module, like a large number of modules in the DeNOx system, had a significant absence of activated carbon at the top of the module.

It is most likely that the reduced NO_2 and NO removal efficiencies were a result of the activated carbon from a large number of modules being progressively lost from the modules during normal operation of the $DeNO_X$ system. The rate of loss of carbon from the modules is currently unknown.

This aspect was investigated further using a “smoke test” where synthetic “smoke” is used to identify gas flow direction. Examples of the results from these investigations are shown in Figure 7.6.

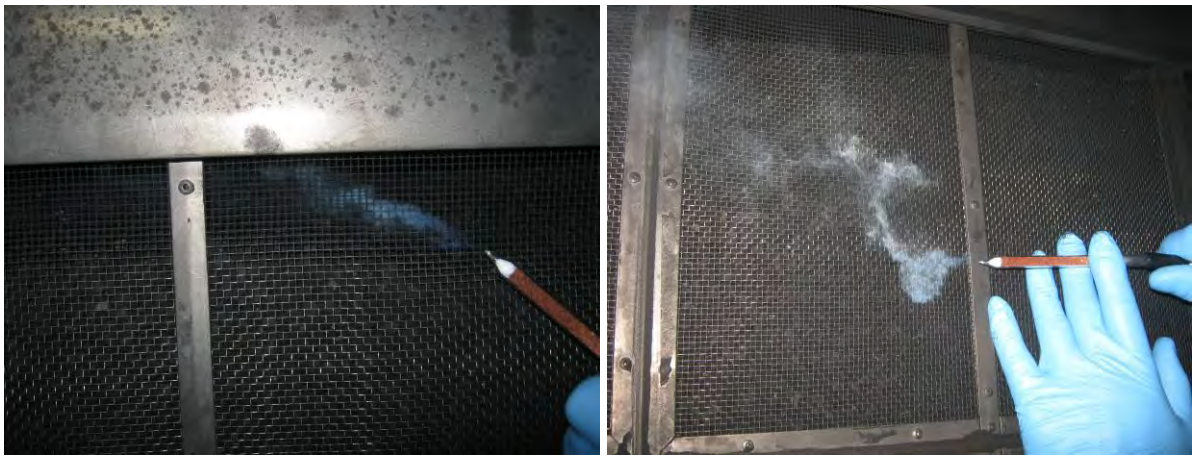

(a) (b)

Figure 7.6. Examples of "Smoke Test" measurements showing the flow path through the Activated Carbon Modules.

Figure 7.6(a) shows a smoke test of a partly filled carbon module and shows that the smoke is strongly drawn into the top section of the module were there is a reduced volume of activated carbon. Figure 7.6(b) shows a similar test but in this case the smoke is directed over the face of the module where the largest mass of carbon is located. During the test shown in Figure 7.6(b) little air was observed to enter the carbon module. These observations clearly indicated that there is significant leakage over the top of the carbon. These observations were repeated and similar smoke behaviour observed for a large number of modules.

The impact of leakage over the activated carbon surface was investigated further by inserting a flow restricting baffle into the airflow above the activated carbon thereby forcing the air to pass through the main body of the activated carbon. The activated carbon sample used for this measurement was a "used" module that had been removed from the DeNOx system. The module with the baffle installed is displayed in Figure 7.7.

Figure 7.7. Insertion of a flow restrictor baffle into top of a carbon module to restrict air leakage over the top of the module.

By installing the flow restrictor that is shown in Figure 7.7 the NO_2 removal efficiency of the "used" activated carbon was increased to 98% and is a NO_2 removal efficiency that is similar to the value for "new" carbon. These measurements suggest that there is little difference between the removal efficiency of "new" and "used" activated carbon.

7.4 NO_2 to NO conversion of activated Carbon.

It was observed that the modules of activated carbon spontaneously produced NO or "off gassed" NO for many hours after being removed from the DeNOx system. The "off gassing" continued after flushing the modules with ambient air at large flow rates and for time periods greater than 12 hours. It is most likely that this is evidence suggesting the existence of an intermediate NO species being formed on the surface of the activated carbon during catalytic conversion of NO_2 to NO. These data suggest that the NO intermediate "off gasses" from the activated carbon as the partial pressure of NO_2 at the active carbon site is reduced. The mechanism for this conversion is documented in the open literature (Guo, Z., et al, 2001; Teng, H., Suuberg, E, M, 1993; Zawadzki, J., Wisniewski, M., Skowronska, K., 2003; Lopez, D., et al 2007)

The spontaneous production of NO was investigated further but for this case "new" activated carbon was used. For this experiment a module of new activated carbon was exposed to a constant 20ppm concentration of NO_2 gas in the ACTA for a period of 12 minutes after which time the NO_2 and air supply were stopped and the NO concentration monitored for the next four hours. The results of these measurements are shown in Figure 7.8.

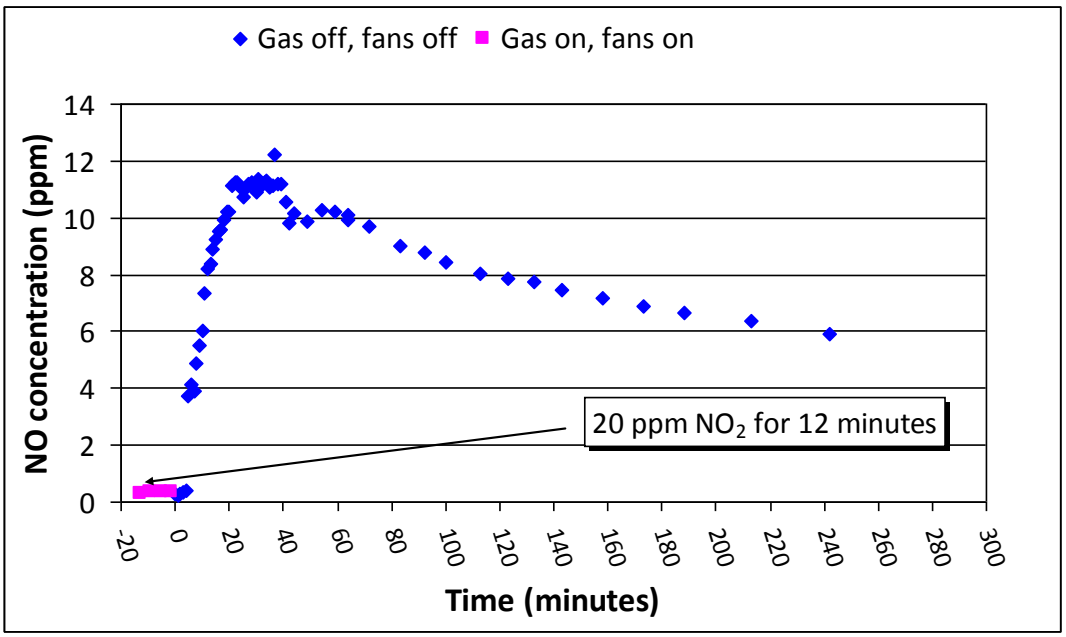

Figure 7.8. Conversion of NO_2 to NO by activated carbon. .

These data displayed in Figure 7.8 display small measured background concentration of NO during the 12 minute period of exposure to 20ppm NO_2. After switching off both the blower and NO_2 gas supply the NO concentration increased quickly to 12 ppm and then slowly decayed to 6ppm after four hours. These data provide strong evidence that the activated carbon is converting NO_2 to NO within the DeNOx system. While further work is required to fully validate the chemistry of these data, these data suggest that the calculated removal efficiency of NO will be influenced by prior exposure of the activated carbon to NO_2. Additionally, this observation gives rise to an alternative method of calculating NO_2 removal efficiency if a nitrogen mass basis is used.

Data shown in Figure 7.8 suggest that the activated carbon is catalytically converting NO_2 to NO and possibly other unidentified species. Scientific literature supports this hypothesis and additionally suggests that while some NO_2 may be retained on the activated carbon in the form of nitric acid, a larger quantity of the NO product will eventually be released from the activated carbon. For the case of the AFP the NO product will be returned to the M5 tunnel. However, this process will be dependent upon the prevailing gas chemistry within the DeNOx.

8 OVERALL CONCLUSION.

CSIRO has undertaken a comprehensive investigation into the DeNOx technology that is installed within the AFP of the M5 tunnel. The primary objective of this study was to determine the NO_2 and NO removal efficiencies of the DeNOx system. The NO_2 and NO removal efficiencies have been determined by both CAPS and CM instrumentation and the most reliable measured NO_2 removal efficiency is 55% a standard deviation of 4%. Hence, the NO_2 removal efficiency is reported as 55% ± 8% with a 95% confidence limit. The most reliable measured NO removal efficiency is 12% with a standard deviation of the order of 5%. The NO removal efficiency is reported as 12% ± 10% with a 95% confidence limit.

A range of additional measurements have been undertaken during these efficiency determinations. These extra measurements have revealed that the activated carbon has the potential for nearly 100% removal of NO_2 from a gas stream for the NO_2 concentrations measured in this study (20ppm). The NO removal efficiency for new activated carbon was measured to be much less than the NO_2 with a removal efficiency of 56%.

The most likely origin of the apparent reduced NO_2 and NO removal efficiency of the DeNOx system compared to “used” activated carbon is from air leakage around and through the activated carbon filled modules.

This study has shown that the NOx mitigation chemistry of activated carbon is complex and much more research is required to fully understand the mechanisms and limitations of this technology within the AFP environment.

9 RECOMENDATIONS.

CAPS instruments were delivered towards the end of this study and as such the performance of these instruments has not been fully evaluated. It is recommended that further research using the CAPS instruments be undertaken to more accurately evaluate the removal efficiency of the DeNOx system.

The NO_2 removal efficiency of activated carbon has been shown to be much greater than the measured NO_2 removal efficiency of the DeNOx system. To increase the NO_2 removal efficiency of the DeNOx system it is suggested that alternative systems be investigated for containing the activated carbon.

9 REFERENCES

Bates, J.N., 1992, „Nitric Oxide Measurements by Chemiluminescence Detection." *Neuroprotocols: A Companion to Methods in Neurosciences*: 1: 141- 149

Clough, P.N., Thrush, B.A., 1967, „Mechanism of Chemiluminescent Reaction between Nitric Oxide and Ozone." *Transactions of the Faraday Society*: 63: 915- 925

Clyne, M.S.A., Thrush, B.A., Wayne, R.P., 1964, „Kinetics of the Chemiluminescent Reaction between Nitric Oxide and Ozone." *Transactions of the Faraday Society*: 60: 359- 370

Glover, J.H., 1975, „Chemiluminescence in Gas Analysis and Flame Spectrometry." *The Analyst*: 100: 449- 463

Guo, Z., Xie, Y., Hong, I., Kim, J., 2001, „Catalytic oxidation of NO to NO_2 on activated carbon." *Energy Conversion and Management*: 42: 2005- 2018

Johnson, H.S., Crosby, H.J., 1954, „Kinetics of the Fast Gas Phase Reaction between Ozone and Nitric Oxide." *Journal of Chemical Physics*: 22: 689- 692

Kang, Y., Kim, J., Son, Y., Kim, P., Chung, S., 2009, „A simultaneous control technology for nitrogen dioxide and toluene in indoor areas." *ICROS-SICE International Joint Conference*: August 18-21 2009, Fukuoka International Congress Center, Japan : 1699- 1702

Kebabian, P.L., Wood, E.C., Herndon, S.C., Freedman, A., 2008 „A Practical Alternative to Chemiluminescence Detection of Nitrogen Dioxide: Cavity Attenuated Phase Shift Spectroscopy" *Environ. Sci. Technol*., 42, 6040-6045,

Kebabian, P.L., Freedman, A., 2007, „System and method for trace species detection using cavity attenuated phase shift spectroscopy with an incoherent light source", U.S. Patent No. 7301639 (issued November 27, 2007).

Kebabian, P.L., Herndon, S.C., Freedman, A., 2005, „Detection of Nitrogen Dioxide by Cavity Attenuated Phase Shift Spectroscopy", *Anal. Chem*., 77, 724-728.

Lee, Y., Choi, D., Hong, I., Park, J., 2002, „Performance of fixed-bed KOH impregnated activated carbon adsorber for NO and NO_2 removal in the presence of oxygen." *Carbon*: 40: 1409- 1417

Lopez, D., Buitrago, R., Sepulveda-Escribano, A., Rodriguez-Reinoso, F., Mondragon, F., 2007, „Low-Temperature Catalytic Adsorption of NO on Activated Carbon Materials." *Langmuir*: 23: 12131- 12137

Teng, H., Suuberg, E, M., 1993, Chemisorption of Nitric Oxide on Char. 2 Irreversible Carbon Oxide Formation." *Ind. Eng. Chem. Res*: 32: 416- 423

Pietrzak, R., 2009, Active Carbons Obtained from Bituminous Coal for NO_2 removal ander Dry and Wet Conditions at Room Temperature." *Energy and Fuels*: 23: 3617- 3624

Zawadzki, J., Wisniewski, M., Skowronska, K., 2003, „Heterogeneous reactions of NO_2 and N0-O_2 on the surface of carbons." *Carbon*: 41: 235- 246

ASTM International, ASTM D 3154 – 00 (Reapproved 2006); “Standard Test Method for Average Velocity in a Duct (Pitot Tube Method)”.

Australian Standard AS 4323.1 - 1995 Stationary source emissions. Method 1: Selection of sampling positions. Standards Australia International Ltd, Sydney

California Environmental Protection Agency. Air Resources Board, Method 1 (1999); “Sample and velocity traverses for stationary sources”.

Hinds, W.C.. (1999) Aerosol Technology, 2th Edition. Wiley Press, New York.

11 APPENDIX 1. GLOSSARY OF TERMS

11.1 Sampling, Aliasing and the Nyquist – Shannon theorem

An analogue signal is any signal where the output variable, such as a voltage, changes continuously with time. Examples include the voltage output of a PMT tube or the voltage change of a battery as it becomes flat. This output can be visualised as a continuous line output on an analogue chart recorder. Analogue signals are different from digital signals. Digital signals are a series of discrete measurements or readings spaced in time. Digital signals are not continuous and must be considered as only as representation of the analogue signal.

Since digital signals are discrete measurements spaced in time, these measurements are interspaced by periods where no measurements are taken. Digital signals are essentially snapshots of the analogue signal. As such, a significant amount of the analogue signal may not be sampled if the snapshot rate is slower than the rate of change of the analogue signal as the “non-sampled” periods mask the analogue signal. Sampling rates smaller than the rate of change of the analogue signal may cause aliasing where the analogue signals are misrepresented by the digital approximation. In the worst case of aliasing the digital output signal becomes a function of the digital sampling time and not the analogue signal.

The Nyquist – Shannon theorem describes the minimum sampling rate that must be used to completely describe an analogue signal where the digital sampling rate must be at lest twice the minimum rate of change of the analogue signal.

12 APPENDIX 2 – EXPERIMENTAL ASSESSMENT OF THE ANCILLARY INSTRUMENT USED FOR THE ASSESSMENT OF THE NOx REMOVAL TECHNOLOGY INSTALLED WITHIN THE AFP.

12.1 Introduction

Prior to and during the NOx removal efficiency measurements undertaken at the AFP the performance of the each of the instruments used to undertake the efficiency determinations were assessed. These instruments included three Environics Series 7000 zero air generators, four Environics Series 6100 multi-gas calibration systems and four Thermo 42i NOx analysers. These comprehensive performance measurements have been used to provide the basis for calculating the uncertainties of the NO, NOx, and NO_2 concentration results as well as the uncertainties of the real time NOx removal efficiency results of the activated carbon installation at the AFP.

The performance of all instruments utilised in the NOx efficiency determinations were initially evaluated under more controlled conditions at CSIRO Laboratories, North Ryde. These initial measurements were supplemented by an ongoing performance assessment program that continued throughout the NOx removal efficiency study at the AFP. These measurements provided an ongoing check of instrumental performance and stability. This appendix presents the findings of these measurements.

The suite of instrument assessment measurements were designed to assess:

a. The quality of the zero air generated by the Environics Series 7000 zero air generators

b. The performance of the Environics Series 6100 multi-gas calibration system including;
    - The linearity of the mass flow controllers
    - Precision of the mass flow controllers on a short term basis (24hr)
    - Long term drift
    - An assessment of the uncertainty of this instrument and measure of the contribution of this uncertainty with respect to the NOx removal efficiency calculations

c. The performance of the Thermo model 42i Chemiluminescent Analysers including;
    - The response of reaction cell to changes in NO concentrations. This has been discussed in Section 4.
    - The linearity of the response signal of each instrument with respect to NO and NO_2.
    - The longer term stability in the response of the instrument with respect to NO and NO_2.
    - Precision of the mass flow controllers on a short term basis (24hr)
    - Long term drift
    - The efficiency of the Molybdenum NOx converters.

These investigations of the Environics Series 7000 zero air generators and Environics Series 6100 multi-gas calibration system are described in the following sections

12.2 Assessment of the Environics Series 7000 zero air generators

NOx free air is required by chemiluminescent analysers to provide a zero or baseline value during calibration measurements. This air was provided by an Environics Series 7000 zero air generator and the quality of this air was assessed both before and during this study by comparing the zero air generated by this instrument to air formed through the recombination of liquid oxygen and nitrogen (Coregas zero grade).

In this validation experiment the zero air form either the Environics Series 7000 generator or Coregas zero air was alternately switched in and out of a sample gas stream to the sample port of a Thermo 42i NOx analyser. The flow of each sample was controlled to maintain a constant pressure and identical gas flow rates at the sample port. The results from these measurements revealed no difference in the baseline or zero concentration within the uncertainty band of the Thermo 41i NOx analyser.

12.3 Assessment of the Environics Series 6100 multi-gas calibration system

All NOx analysers were calibrated against traceable calibration gases (Coregas, NATA traceable specialty gas). Environics Series 6100 multi-gas calibrators were used in conjunction with an Environics Series 7000 zero air generator to dilute the reference gas to useable concentrations for each instrument and to generate constant gas flows. The Environics calibrator incorporates two mass flow controllers to accomplish dilution and mixing operations. This instrument was a critical component in the calibration process and the uncertainties associated with these instruments are directly reflected in the overall uncertainties of the NOx concentration readings and ultimately the NOx removal efficiency estimation. As such, the performance and uncertainties of these instruments was experimentally assessed.

The linearity in flow of the mass flow controllers of each Environics Series 6100 calibrator were compared to a primary flow calibrator (Bios, Defender model 510M, 510H). The results of this investigation are shown in Figure 12.1.

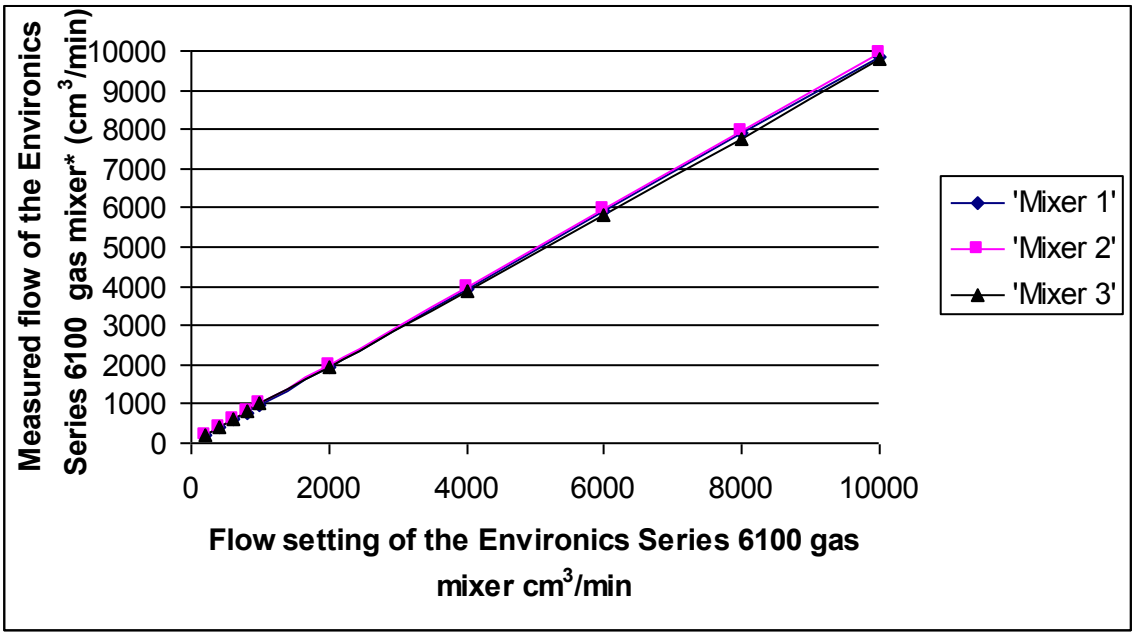

Figure 12.1. Linearity and accuracy of the Environics Series 6100 multi-gas calibrators.

Linearity measurements, precision and long term stability measurements were completed for each of the three Environics Series 6100 multi-gas calibrators. For each measurement the flow delivered by the mass flow controller was compared to the primary flow calibrator (Bios, Defender model 510M, 510H). These data were used to assess the overall contributions of these instruments to the NO_2 removal efficiency measurements. These uncertainties ranged from 3% for mixers indentified as “mixer 2” and “mixer 3” and 7% for “mixer 1”.